Stem Cell Reports
Article

ISSCR

OPEN ACCESS

Sepsis Induces Hematopoietic Stem Cell Exhaustion and Myelosuppression through Distinct Contributions of TRIF and MYD88

Huajia Zhang,[1,2] Sonia Rodriguez,[2] Lin Wang,[2] Soujuan Wang,[3] Henrique Serezani,[3] Reuben Kapur,[2] Angelo A. Cardoso,[2] and Nadia Carlesso[1,2,*]

[1]Department of Medical and Molecular Genetics, School of Medicine, Indiana University School of Medicine, Indianapolis, IN 46202, USA
[2]Herman B Wells Center for Pediatric Research, School of Medicine, Indiana University School of Medicine, 1044 West Walnut, Indianapolis, IN 46202, USA
[3]Department of Microbiology, School of Medicine, Indiana University School of Medicine, Indianapolis, IN 46202, USA
*Correspondence: ncarless@iu.edu
http://dx.doi.org/10.1016/j.stemcr.2016.05.002

SUMMARY

Toll-like receptor 4 (TLR4) plays a central role in host responses to bacterial infection, but the precise mechanism(s) by which its downstream signaling components coordinate the bone marrow response to sepsis is poorly understood. Using mice deficient in TLR4 downstream adapters MYD88 or TRIF, we demonstrate that both cell-autonomous and non-cell-autonomous MYD88 activation are major causes of myelosuppression during sepsis, while having a modest impact on hematopoietic stem cell (HSC) functions. In contrast, cell-intrinsic TRIF activation severely compromises HSC self-renewal without directly affecting myeloid cells. Lipopolysaccharide-induced activation of MYD88 or TRIF contributes to cell-cycle activation of HSC and induces rapid and permanent changes in transcriptional programs, as indicated by persistent downregulation of *Spi1* and *CebpA* expression after transplantation. Thus, distinct mechanisms downstream of TLR4 signaling mediate myelosuppression and HSC exhaustion during sepsis through unique effects of MyD88 and TRIF.

INTRODUCTION

In the adult, the bone marrow (BM) is the central organ for blood production, generating a large number of mature circulating cells daily from a small number of hematopoietic stem cells (HSC). During bacterial infection, BM HSC are challenged with the need of expanding progenitor cell pools to replenish the mature immune cells required to fight the pathogens, in particular neutrophils. Sepsis is one of the most dramatic examples of inadequate host BM response to infection, whereby an initial neutrophilia and hyper-reactive immune response is followed by profound neutropenia, leukocyte hyporesponsiveness, and consequently an inability of the host to control the bacterial infection (Bosmann and Ward, 2013; Hotchkiss and Karl, 2003). The incidence of sepsis is rising, due to increased longevity of patients with chronic diseases and antibiotic-resistant organisms. Even though significant efforts have been made to improve treatment of patients with sepsis, no effective therapy is available and mortality rates remain very high (28%–50%) (Angus, 2011). Hence, novel ideas and approaches are sorely needed to address this significant health problem.

Despite the critical role of the BM during infection, the contribution of BM failure to morbidity and mortality in sepsis has not been fully recognized. Mechanism(s) causing HSC dysfunction in this clinical setting remain elusive. Using an animal model of sepsis and endotoxemia induced by *Pseudomonas aeruginosa* or by its lipopolysaccharide (LPS), we previously demonstrated that HSC act as a direct pathogen stress sensor through activation of Toll-like receptor 4 (TLR4) (Rodriguez et al., 2009; Weighardt and Holzmann, 2007). In this model, HSC undergo dysfunctional expansion in the BM, which is associated with a block of myeloid differentiation and neutropenia in a TLR4-dependent manner. Furthermore, we observed that acute exposure of HSC to LPS permanently affects their ability to engraft and self-renew. A subsequent study also showed that chronic activation of TLR4 impairs HSC functions (Esplin et al., 2011). Collectively, this indicates a broad role of TLR4 in the regulation of hematopoietic homeostasis under stress conditions.

TLR4 recognizes the LPS component of Gram-negative bacteria such as *P. aeruginosa*, *Salmonella*, and *Escherichia coli* (O'Neill and Bowie, 2007), which account for ~60% of sepsis cases (Vincent et al., 2009). Activation of TLR4 by its ligand LPS sets off intracellular signaling through two different adaptors: myeloid differentiation factor 88 (MYD88) and TIR-domain-containing adapter-inducing interferon β (TRIF) (Kawai et al., 2001; Weighardt et al., 2004). The MYD88-dependent pathway activates nuclear factor κB (NF-κB) and activator protein 1 (AP-1), in a manner dependent on mitogen-activated protein kinases (ERKs1/2, JNK, and p38), converging in pro-inflammatory programs. On the other hand, the TRIF pathway activates interferon regulator factor 3 (IRF-3), which induces interferon β (IFN-β) production, also responsible for late activation of NF-κB (Kawai et al., 2001; Yamamoto et al., 2003). Genetic targeting of TLR4, MYD88, and TRIF has demonstrated the complexity of these delicate regulatory pathways during immune response, revealing both deleterious and protective roles of these molecules during severe

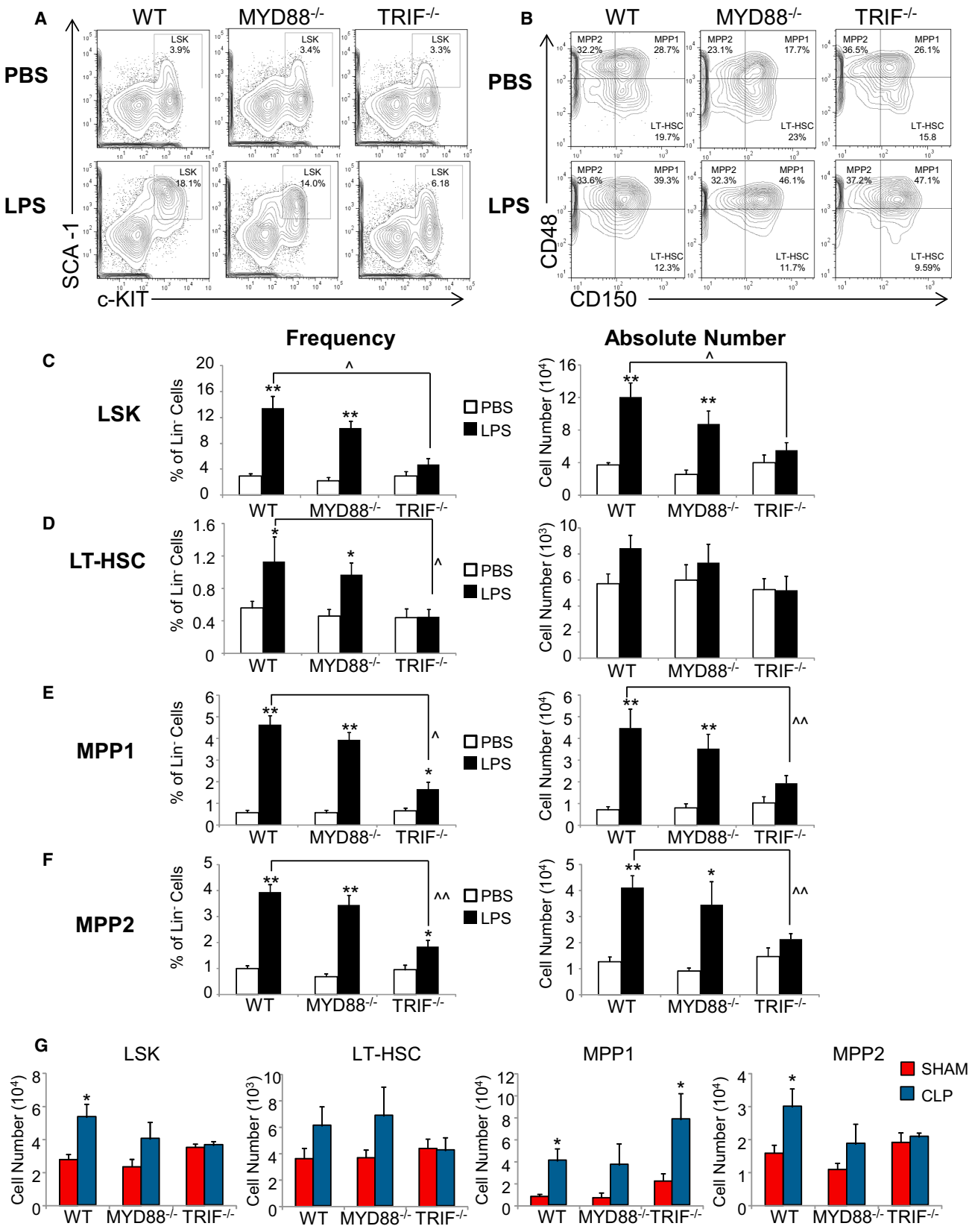

(legend on next page)

bacterial infection. Thus, significant challenges remain for the therapeutic targeting of TLR4 signaling during sepsis (Weighardt et al., 2002). TLR4 and its co-receptor MD2 are expressed in HSC (Nagai et al., 2006), but the functional role of TLR4 downstream signaling in HSC remains unclear. Although a considerable number of studies have investigated the role of MYD88 or TRIF in response to bacterial infections (Roger et al., 2009), it is largely unknown how each pathway affects the function of HSC and progenitors. Hypothesizing that both MYD88 and TRIF are critical during the BM response against bacterial infections, we determined their distinct contributions to HSC and progenitor regulation. We show that during sepsis, MYD88 plays a dominant role in myelosuppression, whereas TRIF mediates persistent injury to HSC functions. These data provide insights into how TLR4 and its adaptors control HSC response to sepsis, thus serving as a guide to define downstream molecules that can be independently targeted to prevent the negative outcomes of severe bacterial infection.

RESULTS

Our previous work showed that severe bacterial sepsis induced by *P. aeruginosa* or by its LPS causes a TLR4-dependent dysfunctional expansion of HSC and hematopoietic progenitor cells (HSPC) (Rodriguez et al., 2009). To determine whether these changes are MYD88 or TRIF dependent, we performed LPS challenge in mice lacking MYD88 ($MYD88^{-/-}$) or TRIF ($TRIF^{-/-}$). Similar to our previous findings, wild-type (WT) mice responded to LPS with a significant increase in the frequency and absolute number of BM $Lin^{-}SCA\text{-}1^{+}c\text{-}KIT^{+}$ (LSK) cells, a subset enriched in HSPC (~4-fold; Figures 1A and 1C). Surprisingly, $TRIF^{-/-}$ mice exhibited no such expansion of LSK cells, whereas $MYD88^{-/-}$ mice behaved in a manner similar to WT mice (Figures 1A and 1C).

The LSK pool can be further dissected by immunophenotypic analysis into distinct subsets (Figure 1B) (Kiel et al., 2005; Wilson et al., 2008), consisting of: long-term HSCs (LT-HSC; $Lin^{-}SCA\text{-}1^{+}c\text{-}KIT^{+}CD150^{+}CD48^{-}$), which have the ability to self-renew; multipotential progenitor 1 cells (MPP1; $Lin^{-}SCA\text{-}1^{+}c\text{-}KIT^{+}CD150^{+}CD48^{+}$), which include short-term HSCs (ST-HSC); and MPP2 cells ($Lin^{-}SCA\text{-}1^{+}c\text{-}KIT^{+}CD150^{-}CD48^{+}$). WT and $MYD88^{-/-}$ mice responded to LPS with a noticeable increase in LT-HSC and a robust expansion (5-fold) of MPP1 and MPP2, in both frequency and absolute number (Figures 1D–1F). In contrast, $TRIF^{-/-}$ mice did not show any noticeable increase in LT-HSC, MPP1, or MPP2 subsets. Of note, following LPS challenge the representation of LT-HSC and MPP within the LSK population shifted in similar manner in all genotypes, with increased representation of MPP1 cells at the expense of LT-HSC (Figure 1B); however, as the total LSK population dramatically increased in WT and $MYD88^{-/-}$ mice, the LT-HSC frequency in the Lin^{-} cell pool and their total absolute number were increased in these genotypes. Overall, there was a trend for increased absolute numbers of LT-HSC (LSK $CD150^{+}CD48^{-}$) in WT mice following LPS, though not statistically significant. Increases in LT-HSC cell numbers were also observed when CD34 and FLK2 were used to define LT-HSC and ST-HSC (Figure S1A), but not when a more stringent definition of the LT-HSC pool was adopted by using SLAM markers in combination with CD244 and CD229 (Oguro et al., 2013) (Figure S1B).

To determine whether these changes were also seen in a bacterial sepsis model, we utilized a mouse model of cecal ligation and puncture (CLP)-induced polymicrobial peritonitis (Ferreira et al., 2014). Responses noted in the LPS model were to a large extent recapitulated in the CLP model (Figure 1G). Modest differences between the models are likely due to the higher complexity of bacterial sepsis compared with LPS challenge. Collectively, these data show that both LPS and bacterial sepsis result in a dramatic increase in MPP1 and MPP2 subsets, associated with no or modest expansion of LT-HSC, and that TRIF, but not MYD88, is required for this process.

Role of SCA-1 Expression and Cell-Cycle Activation in LPS-Induced LSK Expansion

Upregulation of stem cell antigen 1 (SCA-1) expression on HSPC (Essers et al., 2009) and contamination of the LSK pool with $Lin^{-}c\text{-}KIT^{+}SCA\text{-}1^{-}$ (LK) progenitors re-expressing SCA-1 have been reported in response to IFN type I

Figure 1. LPS and Sepsis Induce HSC Expansion in a TRIF-Dependent Manner

Immunophenotypic analysis of BM cells was conducted by fluorescence-activated cell sorting (FACS) on WT, $MYD88^{-/-}$, and $TRIF^{-/-}$ mice 24 hr after challenge with LPS or PBS, or CLP surgery.

(A and B) Representative contour plots for LSK populations (A) or HSPC (B) labeled with SLAM marker (LT-HSC: $Lin^{-}SCA\text{-}1^{+}c\text{-}KIT^{+}CD150^{+}CD48^{-}$; MPP1: $Lin^{-}SCA\text{-}1^{+}c\text{-}KIT^{+}CD150^{+}CD48^{+}$; MPP2: $Lin^{-}SCA\text{-}1^{+}c\text{-}KIT^{+}CD150^{-}CD48^{+}$).

(C–F) Average frequency of LSK (C), LT-HSC (D), MPP1 (E), and MPP2 (F) in the gated Lin^{-} population (left) and average absolute cell number per femur of each subset (right) in PBS- versus LPS-challenged mice (n = 5–14).

(G) Average absolute number of cells per femur in CLP-challenged versus sham-treated mice in BM subsets, from left to right: LSK, LT-HSC, MPP1, and MPP2 (WT: n = 6–11; $MYD88^{-/-}$ and $TRIF^{-/-}$: n = 3–5).

Data represent mean ± SEM. LPS versus PBS: *p < 0.05, **p < 0.01; WT versus $MYD88^{-/-}$ or $TRIF^{-/-}$: ^p < 0.05, ^^p < 0.01.

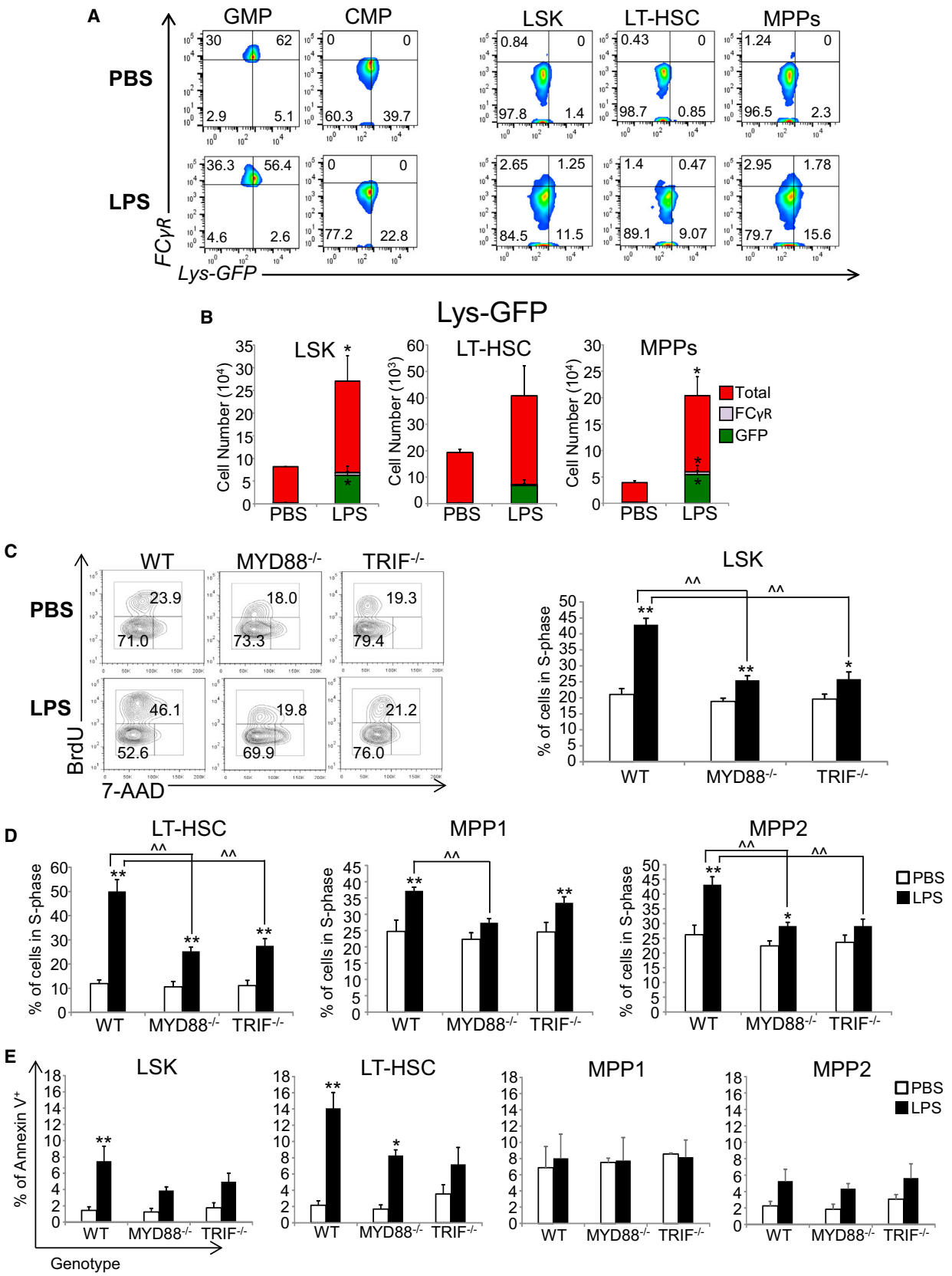

(legend on next page)

exposure (Pietras et al., 2014). In our study, SCA-1 upregulation following LPS occurred mostly on the MPP (MPP1 and MPP2) subsets, and was observed in WT and MYD88$^{-/-}$ mice, but not in TRIF$^{-/-}$ mice (Figure S2A). To determine whether the LSK expansion observed in our model was due to Sca-1 re-expression on more committed progenitors, we tracked the expression of lysozyme-M (Lys) and FCγR in LSK cells in response to LPS. In Lys-GFP transgenic mice (Faust et al., 2000), GFP is under control of the lysozyme promoter, whose activation is increased during myeloid differentiation. Thus, Lys-GFP is highly expressed in myeloid progenitors, in particular in common myeloid progenitor (CMP) and granulocyte-monocyte progenitor (GMP), whereas its expression is minimal in LSK cells (Miyamoto et al., 2002). Similarly, FCγR is highly expressed in GMP and myeloid progenitors. We reasoned that if LSK expansion was due to SCA-1 re-expression by myeloid progenitors, the LSK subset would show a dominant representation of Lys-GFP- and FCγR-expressing cells following LPS challenge. LSK cells from the LPS-challenged mice (defined hereafter as LPS LSK cells) showed a higher content of Lys-GFP and FCγR expression compared with LSK cells from control PBS mice (defined hereafter as PBS LSK cells), especially in the MPP fraction (Figures 2A, S2B, and S2C); however, increases in absolute numbers were modest (Figure 2B). Total numbers of Lys-GFP cells were reduced within the overall Lin$^-$c-KIT$^+$ population (including SCA-1$^+$ and SCA-1$^-$ cells) following LPS (Figure S2D). This is in agreement with our collective observations that severe sepsis or LPS inhibits differentiation and reduces output of myeloid cells. Of note, Lys-GFP fluorescent intensity was not directly affected by LPS (Figure S2E). Comparison of FCγR expression in the LSK subsets of WT, MYD88$^{-/-}$, and TRIF$^{-/-}$ showed no noticeable differences among different genotypes (Figure S2F). Taken together, these data indicate that contamination of the LSK pool by more differentiated cells re-expressing SCA-1 contributes only in part to the cell expansion of primitive cells observed following LPS.

In vivo cell-cycle analysis showed that LPS challenge induced cell-cycle activation in the primitive cell subsets of all genotypes (Figures 2C and 2D). Following LPS, the fraction of cycling LT-HSC was increased 5-, 2-, and 3-fold, respectively in WT, MYD88$^{-/-}$, and TRIF$^{-/-}$ mice. Interestingly, cycling of MYD88$^{-/-}$ and TRIF$^{-/-}$ HSPC was increased in a similar manner following LPS, despite their different expansion responses. Cell-cycle activation induced by LPS was associated with an increase in apoptosis, which was more noticeable in WT cells; similar rates of apoptosis in response to PBS and LPS were observed in MPP cells in all genotypes (Figure 2E).

Loss of MYD88 Rescues LPS-Induced Myelosuppression

Consistent with our previous results (Rodriguez et al., 2009), acute exposure to *P. aeruginosa* LPS caused a significant reduction of BM CMP, GMP, and GR1$^+$MAC1$^+$ subsets without affecting CLP (Figures 3A–3E, S3A, and S3B). Strikingly, loss of MYD88, but not TRIF, prevented reduction of these subsets (Figures 3C–3E). Myeloid progenitors showed modest changes in the cell cycle following LPS (Figure S3C). Apoptosis was significantly increased in WT CMP, GMP, and GR1$^+$MAC1$^+$ cells whereas it was modestly augmented in MYD88$^{-/-}$ and TRIF$^{-/-}$ CMP, and negligible in the GMP cell populations (Figure S3D). These results suggest that the protective effect of MYD88 deficiency on myelosuppression cannot be explained simply by reduced apoptosis and/or increased cell cycle, and that other mechanisms contribute to this process.

These effects were also recapitulated in a mouse model of bacterial sepsis. Similarly to what was observed upon LPS administration, myeloid progenitors and mature myeloid cells were dramatically reduced during CLP-induced peritonitis; this effect was prevented by loss of MYD88, but not loss of TRIF (Figure 3F). Collectively, these data show that activation of the TLR4-MYD88 pathway plays a dominant role in mediating myeloid suppression during endotoxemia and sepsis.

Cell-Autonomous and Non-Cell-Autonomous Effects of TRIF and MYD88 on HSC and Myeloid Progenitors during Sepsis

In addition to mechanisms intrinsic to hematopoietic cells, the microenvironment regulates hematopoiesis through inflammatory cytokines secreted by non-hematopoietic cells (van Lieshout et al., 2012). Thus, we evaluated the

Figure 2. Role of SCA-1 Re-expression, Cell-Cycle Activation, and Cell Survival in LSK Expansion following LPS

(A and B) Lys-GFP reporter mice were challenged with LPS or PBS and their BM analyzed by FACS at 24 hr. (A) Representative density plots for Lys-GFP and FCγR expression on GMP, CMP, LSK, LT-HSC, and MPP subsets in the BM. (B) Absolute number per femur of total (red), FCγR$^+$ (purple), and Lys-GFP$^+$ (green) cells in LSK (left), LT-HSC (middle), and MPP (right) subsets (n = 3–4).

(C–E) Analysis of the BM after 24 hr of LPS or PBS challenge in WT, TRIF$^{-/-}$, and MYD88$^{-/-}$ mice. (C) Representative contour plots (left) showing S phase (as bromodeoxyuridine incorporation) and G_0/G_1 phase for the LSK population. Bar graph (right) indicates the mean LSK distribution in S phase and G_0 phase (n = 16–20). (D) Bar graphs show the percentage of cells in S phase in LT-HSC, MPP1, and MMP2 (n = 7–10). (E) Bar graphs show the percentage of annexin V$^+$ cells in LSK, LT-HSC, MPP1, and MMP2 (n = 3–5).

Data represent mean ± SEM. LPS versus PBS: *p < 0.05, **p < 0.01; WT versus MYD88$^{-/-}$ or TRIF$^{-/-}$: ^^p < 0.01.

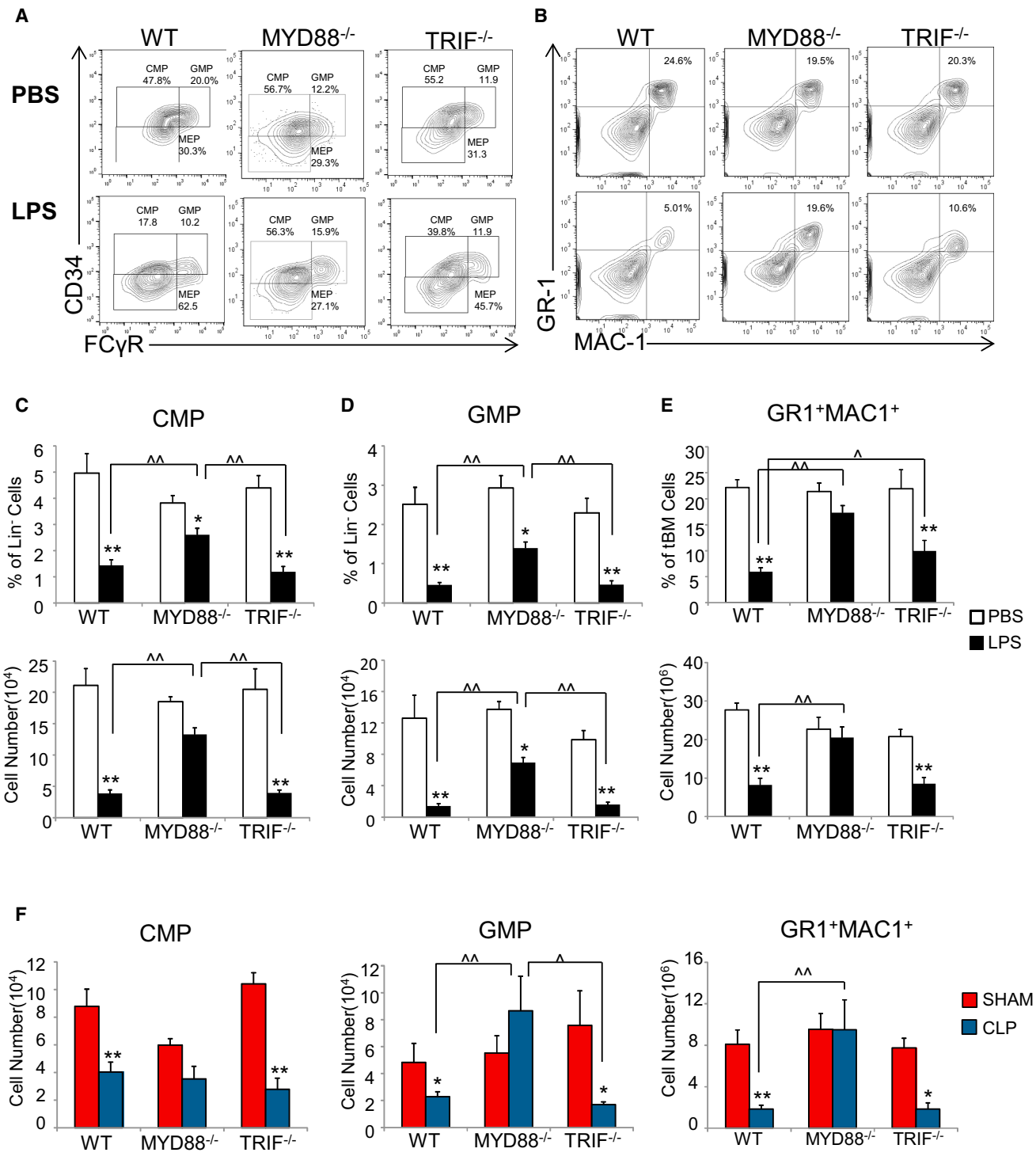

Figure 3. LPS and Sepsis Induce BM Myeloid Suppression in an MYD88-Dependent Manner

Immunophenotypic analysis of BM cells was conducted by FACS on WT, MYD88$^{-/-}$, and TRIF$^{-/-}$ mice 24 hr after challenge with LPS or PBS, or CLP surgery.

(A) Representative contour plots of myeloid progenitor populations labeled with the progenitor markers (CMPs: Lin^{-}IL-7Rα^{-}SCA-1^{-}c-KIT^{+}CD34^{+}FCγR^{lo}; GMPs: Lin^{-}IL-7Rα^{-}SCA-1^{-}c-KIT^{+}CD34^{+}FCγR^{hi}; MEPs: Lin^{-}IL-7Rα^{-}SCA-1^{-}c-KIT^{+}CD34^{-}FCγR^{lo}).

(B) Representative contour plots of mature myeloid GR1^{+}MAC1^{+} cells.

(legend continued on next page)

role of tumor necrosis factor α (TNF-α), granulocyte colony-stimulating factor (G-CSF), and IFN-α, cytokines that are consistently upregulated during infections by LPS (Boettcher et al., 2014; Weighardt and Holzmann, 2007). The effects of LPS on BM LSK and GR1$^+$MAC1$^+$ pools were recapitulated by in vivo injection of recombinant TNF-α (Figure S4A) and were IFN type I independent, as shown by the impact of LPS stimulation in *Ifnar1*$^{-/-}$ mice (Figure S4B). Following LPS challenge, MYD88$^{-/-}$ mice were defective in production of G-CSF and TNF-α, whereas TRIF$^{-/-}$ mice were defective only in TNF-α production (Figure S4C). While IFN-α serum levels were greatly induced by polyinosinic:polycytidylic acid (pIpC), they were modestly upregulated by LPS in WT mice and were close to normal in both MYD88$^{-/-}$ and TRIF$^{-/-}$ mice, despite their different responses to LPS (Figure S4D). Thus, in TRIF$^{-/-}$ mice LPS-induced myelosuppression still occurs despite low levels of TNF-α and IFN-α, and LPS-induced LSK expansion is abrogated despite high levels of G-CSF, suggesting that additional mechanisms contribute to this complex process.

To dissect the relative contribution of cell-autonomous and non-cell-autonomous mechanisms mediated by MYD88 and TRIF, we established two BM chimeric mouse models: (1) CD45.2$^+$ TRIF$^{-/-}$ or MYD88$^{-/-}$ BM donor cells engrafted into CD45.1$^+$ WT recipient mice, and vice versa; and (2) mixed chimeras: CD45.2$^+$ WT-GFP BM cells mixed 1:1 with CD45.2$^+$ TRIF$^{-/-}$ or MYD88$^{-/-}$ cells engrafted into CD45.1$^+$ WT recipient mice (Figure S4E). These mice were challenged with LPS at 8–10 weeks after transplantation, when donor cells were fully engrafted (>80%, data not shown). Analysis of the HSC populations in the reciprocal chimeras showed that loss of TRIF was protective when it was occurring in either the hematopoietic cells or the microenvironment (Figure 4A). The mixed chimeras confirmed that the hematopoietic-restricted effect observed in TRIF$^{-/-}$ LT-HSC and MPP was cell intrinsic and not due to soluble factors secreted by WT hematopoietic cells acting in *trans* (Figure 4B and scheme in Figure 4F). As expected, loss of MYD88 did not affect HSC expansion in any of the chimeras (Figures 4B and S4F). In contrast, loss of MYD88, but not of TRIF, protected GMP and GR1$^+$MAC1$^+$ cells from the effects of LPS, when it was occurring both in the hematopoietic cells and in the microenvironment (Figures 4C and 4D). Experiments conducted with the mixed chimeras demonstrated that the protection conferred to GR1$^+$MAC1$^+$ cells by MYD88 deletion was abolished in the presence of WT hematopoietic cells. This indicates that factors secreted by hematopoietic cells acting in *trans* contributed to the hematopoietic-restricted effect of MYD88 on GR1$^+$MAC1$^+$ cells (Figures 4E and 4F).

Distinct Impact of MYD88 and TRIF on Myeloid Progenitor Differentiation

Direct LPS stimulation of Lin$^-$ cells in vitro resulted in expansion of LSK cells and decreases in myeloid progenitors and GR1$^+$MAC1$^+$ cells (Figures 5A and S5A). This confirmed the contribution of a hematopoietic-restricted mechanism that was microenvironment independent.

Comparative analysis of *Tlr4*, *Trif*, and *Myd88* showed a comparable pattern of expression in WT LSK, CMP, GMP, and GR1$^+$MAC1$^+$ subsets (Figure S5B), suggesting that the differential impact of TRIF and MYD88 on various BM subsets is independent of their relative expression level, and likely due to the different cell context. To further investigate differences exhibited by the WT, MYD88$^{-/-}$, and TRIF$^{-/-}$ myeloid progenitors during sepsis, we examined their ability to differentiate in vitro after in vivo exposure to LPS. CMP and GMP subsets were sorted from each genotype following PBS or LPS challenge and grown in vitro in conditions favoring myeloid differentiation. Sorted CMP from LPS-challenged WT and TRIF$^{-/-}$ mice exhibited defective differentiation into GR1$^+$MAC1$^+$ cells compared with CMP from PBS controls. In contrast, CMP from LPS-treated MYD88$^{-/-}$ mice differentiated similarly to PBS controls (Figure 5B). Differentiation of GMPs into GR1$^+$MAC1$^+$ cells was similar in both conditions (Figure 5C). These data show that in response to LPS, activation of MYD88, but not TRIF, impairs CMP differentiation into GR1$^+$MAC1$^+$ cells.

Loss of TRIF Protects HSC from the Exhaustion Induced by Endotoxemia

Bacterial sepsis causes dysfunctional expansion of HSPC followed by their exhaustion and inability to reconstitute recipients over short and long terms (Rodriguez et al., 2009). As the loss of TRIF, but not MYD88, prevented expansion of immunophenotypic HSPC following LPS challenge or sepsis, we investigated whether loss of TRIF could also prevent the HSC exhaustion observed in transplantation assays. CD45.2$^+$ LSK cells (n = 2,500) sorted from the BM of PBS- or LPS-challenged WT, MYD88$^{-/-}$, or TRIF$^{-/-}$ mice were transplanted into lethally irradiated CD45.1$^+$ recipients together with 10^5 whole BM competitor cells (CD45.1$^+$). PBS LSK pools containing comparable

(C–E) Average frequency (top) of CMP (C) and GMP (D) in the gated Lin$^-$ population and of GR1$^+$MAC1$^+$(E) in the total BM population, and average absolute cell number per femur of each subset (bottom) in PBS- versus LPS-challenged mice (n = 5–14).
(F) Bar graphs indicate the mean of absolute number of CMP, GMP, and GR1$^+$MAC1$^+$ per femur in mice subjected to CLP- versus sham-treated mice (WT and MYD88$^{-/-}$: n = 6–10; TRIF$^{-/-}$: n = 3).
Data represent mean ± SEM. LPS versus PBS: *p < 0.05, **p < 0.01; WT versus MYD88$^{-/-}$ or TRIF$^{-/-}$: ^p < 0.05, ^^p < 0.01.

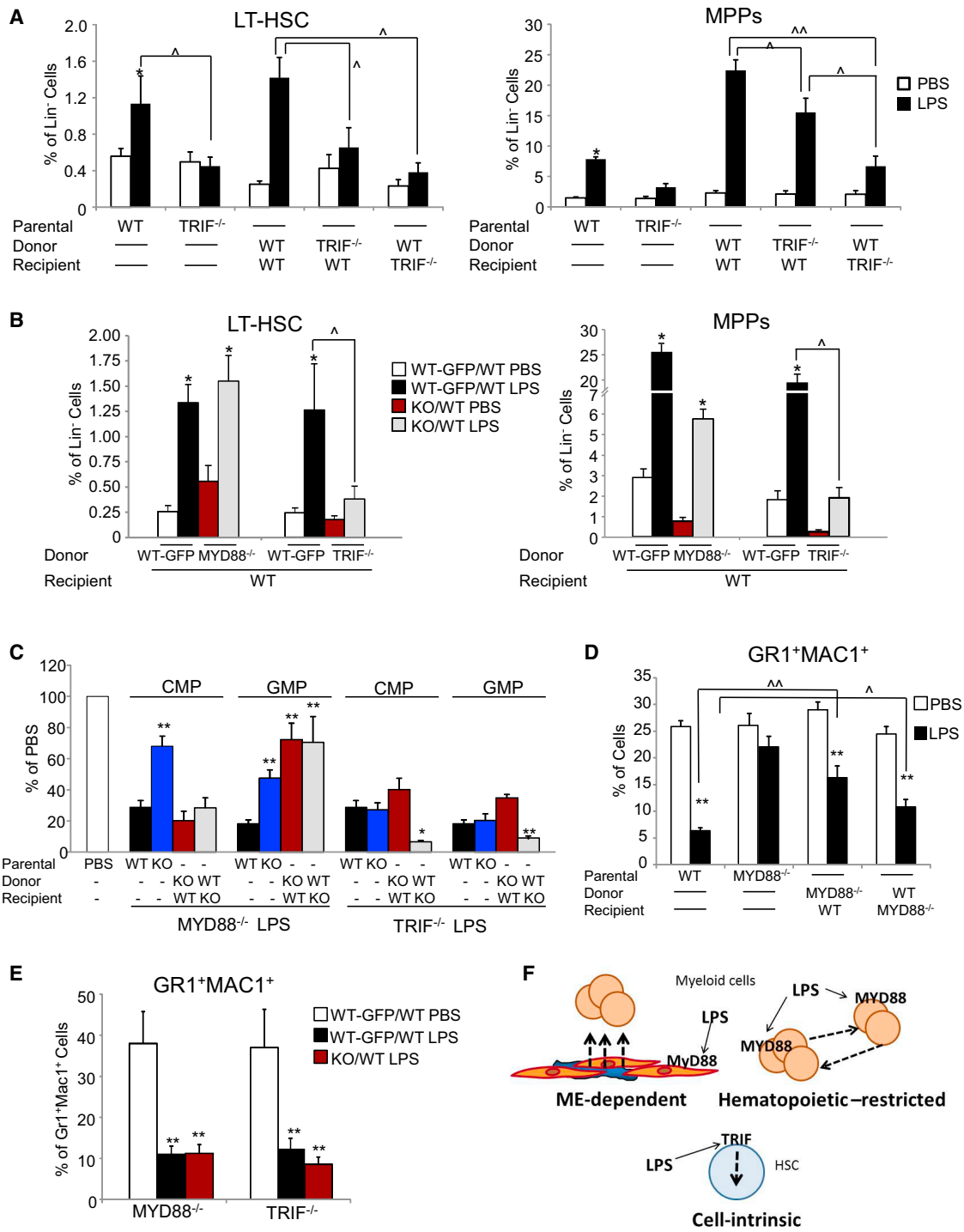

Figure 4. Cell-Autonomous and Non-cell-autonomous Roles of TRIF and MYD88 in LPS-Induced HSC Expansion and Myelosuppression

(A) Chimeras: WT recipients of TRIF$^{-/-}$ donor cells, TRIF$^{-/-}$ recipients of WT donor cells, and WT recipients of WT cells were challenged with LPS or PBS and analyzed after 24 hr (n = 4). WT and TRIF$^{-/-}$ mice (parental) were used as a reference (n = 11). Bar graph shows the mean percentage of LT-HSC and MPPs in the Lin^{-} population.

(B) WT recipients (CD45.1) were transplanted with WTGFP^{+} + MYD88$^{-/-}$ BM cells or WTGFP^{+} + TRIF$^{-/-}$ BM cells, mixed 1:1 ratio. After 8 weeks mice were challenged with LPS or PBS for 24 hr. Bar graphs show the mean percentage of LT-HSC and MPPs in gated WTGFP^{+} donor cells (light and dark gray bars, n = 4) and in gated GFP^{-} (CD45.2) KO donor cells (red and black bars, n = 4) within the same recipient.

(legend continued on next page)

numbers of LT-HSC (range 400–512) and MPP (range 1,351–1,391) in all genotypes engrafted equally well over short and long terms (~70% chimerism at 24 weeks; Figure 6A, left panel). In contrast, LPS LSK pools from WT, MYD88$^{-/-}$, and TRIF$^{-/-}$ mice containing a comparable number of LT-HSC (range 211–229) and MPP (range 1,665–1905) displayed significant differences in their ability to compete and engraft over the short and long terms (Figure 6A, right panel). The engraftment ability of LPS WT LSK was poor over both short and long terms: chimerism ranged from 10% at week 8 to 15% at week 24. Importantly, low engraftment of septic WT cells was not due to decreased homing (Figure 6B). This indicates that despite LT-HSC numbers were not significantly perturbed, and MPP numbers were increased after LPS, their short- and long-term ability to reconstitute hematopoiesis was severely impaired. In contrast, LPS-treated TRIF$^{-/-}$ LSK cells showed significantly improved short-term engraftment (51% chimerism at week 8), and fully restored long-term reconstitution at 24 weeks (68% chimerism; Figure 6A). LPS MYD88$^{-/-}$ LSK cells showed engraftment between that of LPS WT and TRIF$^{-/-}$ LSK cells (22% chimerism at week 8 and 35% at week 24).

Analysis of total BM at week 24 after transplantation showed that LPS LSK from WT donor mice contributed only to 35% of all recipients' BM, whereas LPS LSK from MYD88$^{-/-}$ and TRIF$^{-/-}$ donors contributed to 47% and 73%, respectively (Figure 6C). Moreover, the contribution of LPS TRIF$^{-/-}$ LSK donor cells to the total recipient LSK pool was similar to that of PBS TRIF$^{-/-}$ LSK donor cells, indicating complete protection by TRIF deletion (Figure S6D). Analysis of primitive subpopulations showed a low contribution of WT and MYD88$^{-/-}$ LPS LSK donor cells to LT-HSC, MPP1, and MPP2 subsets (ranging from 13% to 38%), whereas TRIF$^{-/-}$ LPS LSK donor cells contributed 60%–80% to all the primitive subsets (Figure 6D).

Next, we measured the impact of acute exposure to LPS on LT-HSC self-renewal. Absolute numbers of donor LT-HSC in recipient BM was evaluated at 24 weeks after transplantation and compared with absolute numbers of LT-HSC in parental mice used as donors (input control; Figure 6E). PBS LT-HSCs from WT, MYD88$^{-/-}$, and TRIF$^{-/-}$ donors maintained a similar regeneration potential at 24 weeks after transplantation and reached total numbers similar to those of each parental mouse. In contrast, LPS-treated WT donor LT-HSC exhibited significantly fewer numbers compared with input control (~5-fold decrease), but LPS-treated TRIF$^{-/-}$ LT-HSC showed a capacity of regeneration similar to PBS-treated TRIF$^{-/-}$ LT-HSC. LPS-treated MYD88$^{-/-}$ LT-HSC showed intermediate regeneration potential. Calculation of the LT-HSC self-renewal quotient, as previously described (Challen et al., 2012), showed that it was greatly decreased in LPS WT LT-HSC, but was highly preserved in LPS TRIF$^{-/-}$ LT-HSC (Figure 6F). In conclusion, these results show that LPS exposure results in qualitative damage to LT-HSC and MPP, and that loss of TRIF protects LT-HSC self-renewal and MPP functions during acute stress.

Impact of Endotoxic Injury on Multilineage Reconstitution and Expression of Key Regulators of HSC Transcriptional Programs

We examined whether LPS alters the ability of HSCs to replenish all hematopoietic lineages and whether MYD88 and/or TRIF deficiency has an impact on this function. WT donor-derived LPS HSC differentiated less into CMP, GMP, megakaryocyte-erythrocyte progenitor (MEP), CLP, and GR1^{+} subsets compared with control PBS HSC (6%–25% overall; Figures 7A and S7A). However, TRIF deficiency rescued the ability of LPS LSK cells to differentiate into these subsets: LPS TRIF$^{-/-}$ donor cells contributed to up to 70% of CMPs, GMPs, and MEPs, 68% of CLPs, and 73% of GR1^{+} subsets. MYD88 deficiency showed some protection, as seen by an increased contribution to CMPs and GMPs (up to 40%), to CLPs and MEPs (up to 27%), and to GR1^{+} cells (up to 56%; Figures 7A and S7A).

(C) Bar graph shows the percentage of CMP and GMP in LPS- versus PBS-treated mice: in chimeras WT recipients of TRIF$^{-/-}$ or MYD88$^{-/-}$ cells, TRIF$^{-/-}$ and MYD88$^{-/-}$ recipients of WT cells, and in parental WT, MYD88$^{-/-}$, and TRIF$^{-/-}$ mice. Parental, n = 8–19; chimeras, n = 4–6.

(D) WT recipients of MYD88$^{-/-}$ donor cells, MYD88$^{-/-}$ recipients of WT donor cells, and parental WT and MyD88$^{-/-}$ mice were challenged with LPS or PBS and analyzed after 24 hr. Bar graph shows the mean percentage of GR1^{+}MAC1^{+} cells in total BM cells (n = 8–17).

(E) WT recipients (CD45.1) were transplanted with WTGFP^{+} + MYD88$^{-/-}$ BM cells or WTGFP^{+} + TRIF$^{-/-}$ BM cells, mixed 1:1 ratio. After 8 weeks mice were challenged with LPS or PBS for 24 hr. Bar graphs show the mean percentage of GR1^{+}MAC1^{+} cells in in gated WTGFP^{+} donor cells (WT; n = 4) and in gated GFP^{-} (CD45.2) KO donor cells (KO, n = 4) within the same recipient. PBS controls are WT-GFP^{+} of all chimeras challenged with PBS (n = 8).

(F) LPS activation of TLR4-MYD88 or -TRIF signaling exerts its effects on hematopoietic cells (HC) through direct and indirect mechanisms: (1) microenvironment-dependent: activation of MYD88 in the BM stroma cells results in the release of factors that act on HC; (2) hematopoietic-restricted: activation of MYD88 in HC stimulates the release of factors affecting neighboring HC in a paracrine fashion; (3) cell-intrinsic (or cell-autonomous): activation of TRIF in the HC causes a direct effect on the cell.

Data represent mean ± SEM. LPS versus PBS: *p < 0.05, **p < 0.01; WT versus MYD88$^{-/-}$ or TRIF$^{-/-}$: ^p < 0.05, ^^p < 0.01.

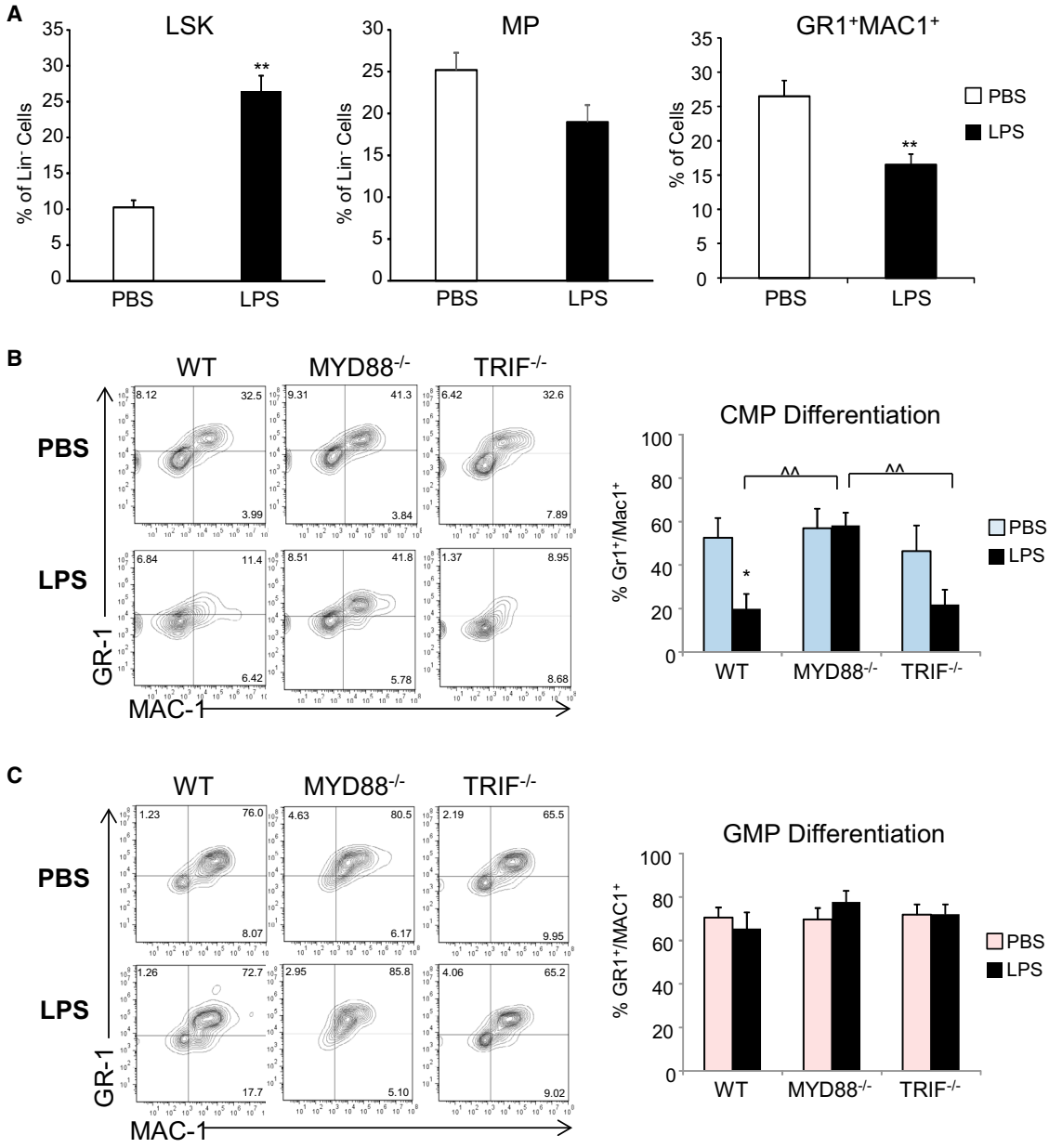

Figure 5. Loss of MYD88 but Not TRIF Preserves Myeloid Differentiation

(A) Purified Lin^- cells were cultured with PBS or LPS in vitro and analyzed 12 hr later. Bar graphs show the percentage of LSK, MP (CMP + GMP) in Lin^- cells, and $GR1^+MAC1^+$ in total alive cells (n = 6).

(B and C) CMP and GMP subsets were sorted from WT, $TRIF^{-/-}$, and $MYD88^{-/-}$ mice exposed to LPS or PBS for 24 hr. Sorted cells were cultured in vitro in myeloid differentiation conditions. Representative contour plots (left) and average percentage (right) of $GR1^+MAC1^+$ cells generated from CMPs at day 4 (B) and from GMPs at day 2 (C) (n = 3–4).

Data represent mean ± SEM. LPS versus PBS: *p < 0.05, **p < 0.01; $MYD88^{-/-}$ versus WT or $TRIF^{-/-}$: ^^p < 0.01.

Analysis of multilineage reconstitution in peripheral blood was consistent with these observations. LPS WT HSC showed a very low contribution to myeloid, B, and T cells at early and late time points. Although overall lineage distribution was not significantly affected, contribution to the myeloid lineage was relatively more compromised in the short term (8 weeks; Figures 7B and S7B), suggesting an impairment of MPP to readily generate myeloid progenitors, as previously observed (Rodriguez et al., 2009). LPS $TRIF^{-/-}$ HSC contributed robustly to all

three lineages at every time point examined (early, 28%–63%; late, 43%–78%), and MYD88$^{-/-}$ LPS HSC showed intermediate engraftment potential, with progressive improvement over time (early, 19%–45%; late, 30%–47%).

To gain further insight into downstream events associated with altered myeloid differentiation and HSC functions during sepsis, we evaluated the expression of two transcription factors critical for HSC and myeloid differentiation programs: PU.1 (encoded by *Spi1*) and C/EBPα (encoded by *CebpA*). qPCR analysis of sorted BM subsets after LPS showed a dramatic decrease in *Spi1* transcripts in WT and TRIF$^{-/-}$ LSK cells, but not in MYD88$^{-/-}$ LSK cells (Figure 7C left). Analysis of PU.1 expression following LPS in the Spi1-GFP reporter mice confirmed its downregulation in LT-HSC and MPP and, in particular, in committed progenitors (Figures S7C–S7E). Similarly, *CebpA* expression was significantly decreased in WT LSK cells following LPS challenge, but remained unaffected in the absence of MYD88 or TRIF (Figure 7C right). Of note, persistence of normal levels of *Spi1* and *CebpA* expression correlated with maintenance of myeloid differentiation in MYD88$^{-/-}$ mice during LPS endotoxemia.

As HSC exposed to LPS showed decreased short- and long-term ability to engraft and differentiate (Figures 7A, 7B, and S7B), we investigated whether changes in *Spi1* and *CebpA* levels observed in response to LPS persisted after transplantation. LPS WT LSK cells sorted at 24 weeks after transplantation exhibited lower expression of both *Spi1* and *CebpA* compared with WT PBS LSK cells. In contrast, MYD88$^{-/-}$ and TRIF$^{-/-}$ LPS LSK cells maintained levels of *Spi1* and *CebpA* expression similar to those of PBS LSK controls (Figure 7D). Collectively, these data suggest that acute LPS exposure leads to long-lasting downregulation of key transcription factors required for HSC maintenance and myeloid differentiation. Loss of TRIF and/or MYD88 partially prevented such disruptions, indicating their association with transcriptional programs regulated by PU.1 and C/EBPα.

DISCUSSION

TLR4 activation via MYD88 or TRIF pathways plays a central role in regulating host defense against bacterial infection (Poltorak et al., 1998; Beutler, 2000; Weighardt and Holzmann, 2007). However, the specific contribution of MYD88 and TRIF in regulating the BM response to sepsis is poorly understood. In this study, we dissected these two pathways using knockout mice lacking MYD88 or TRIF function in combination with *P. aeruginosa* LPS-induced endotoxemia (Rodriguez et al., 2009) or CLP-induced peritoneal polymicrobial sepsis (Ferreira et al., 2014). Our observations unveil two distinct mechanisms mediating the effects of severe sepsis on BM homeostasis. MYD88 activation is critical for myelosuppression occurring in BM during sepsis, whereas TRIF activation mediates permanent injury of HSC (Figure 7E).

Based on our previous findings (Rodriguez et al., 2009), we initially hypothesized that the myelosuppression occurring during sepsis was caused by dysfunctional expansion of HSPC (LSK) associated with a block of differentiation and inability to produce adequate myeloid precursors. However, our studies using MYD88$^{-/-}$ and TRIF$^{-/-}$ mice suggest that myelosuppression and HSPC dysfunction can occur as two independent processes. Analysis of BM response to LPS challenge or severe sepsis showed that TRIF deficiency prevented LSK expansion, but not the loss of myeloid progenitors. In contrast, MYD88 deficiency preserved myeloid cells but did not abolish the LSK expansion. This suggests that TRIF and MYD88 have cell-specific effects.

Following LPS or sepsis CMP and GMP pools are rapidly depleted, resulting in decreased output of GR1^{+}MAC1^{+} cells, an effect largely prevented by loss of MYD88 but not of TRIF. Differences in cell cycle and apoptosis of myeloid progenitors in the three genotypes did not sufficiently account for differences in outcome. Indeed, we observed that CMP's ability to differentiate into mature GR1^{+}MAC1^{+} cells was severely impaired following in vivo exposure to LPS, and that this effect was MYD88 dependent. Reciprocal transplants showed that deletion of MYD88 prevented myelosuppression by the combinatorial effect of microenvironment-dependent and -independent mechanisms (hematopoietic-restricted). Mixed chimera experiments demonstrated that the hematopoietic lineage-restricted effect of MYD88 on GR1^{+}MAC1^{+} cells is mediated by secondary factor(s) produced by hematopoietic cells and acting in *trans* on myeloid cells. It is likely that cytokines such as TNF-α, INFs, and G-CSF contribute to MYD88-dependent myelosuppression following LPS. In vivo inoculation of recombinant TNF-α reduced GR1^{+}MAC1^{+} cells in a manner similar to that under LPS challenge. However, GR1^{+}MAC1^{+} cell production following LPS was severely hampered in TRIF$^{-/-}$ and *Ifnar1*$^{-/-}$ mice despite a low level of TNF-α and dampened IFN-α response, suggesting as yet unidentified additional players contributing to this process.

Thus, whereas MYD88 has a protective effect in chronic inflammation (Boettcher et al., 2014), it has an adverse effect on myeloid cells during severe sepsis (see notes in Figure S4).

As previously reported (Rodriguez et al., 2009), we observed a significant expansion of immunophenotypically defined LSK cells following LPS stimulation or CLP-induced peritonitis. This increase in the LSK subset was mostly due to expansion of the MPP pool. A modest increase in LT-HSC numbers was observed when LT-HSC were defined as LSK CD150^{+}CD48^{-} (used for this study), while there was a

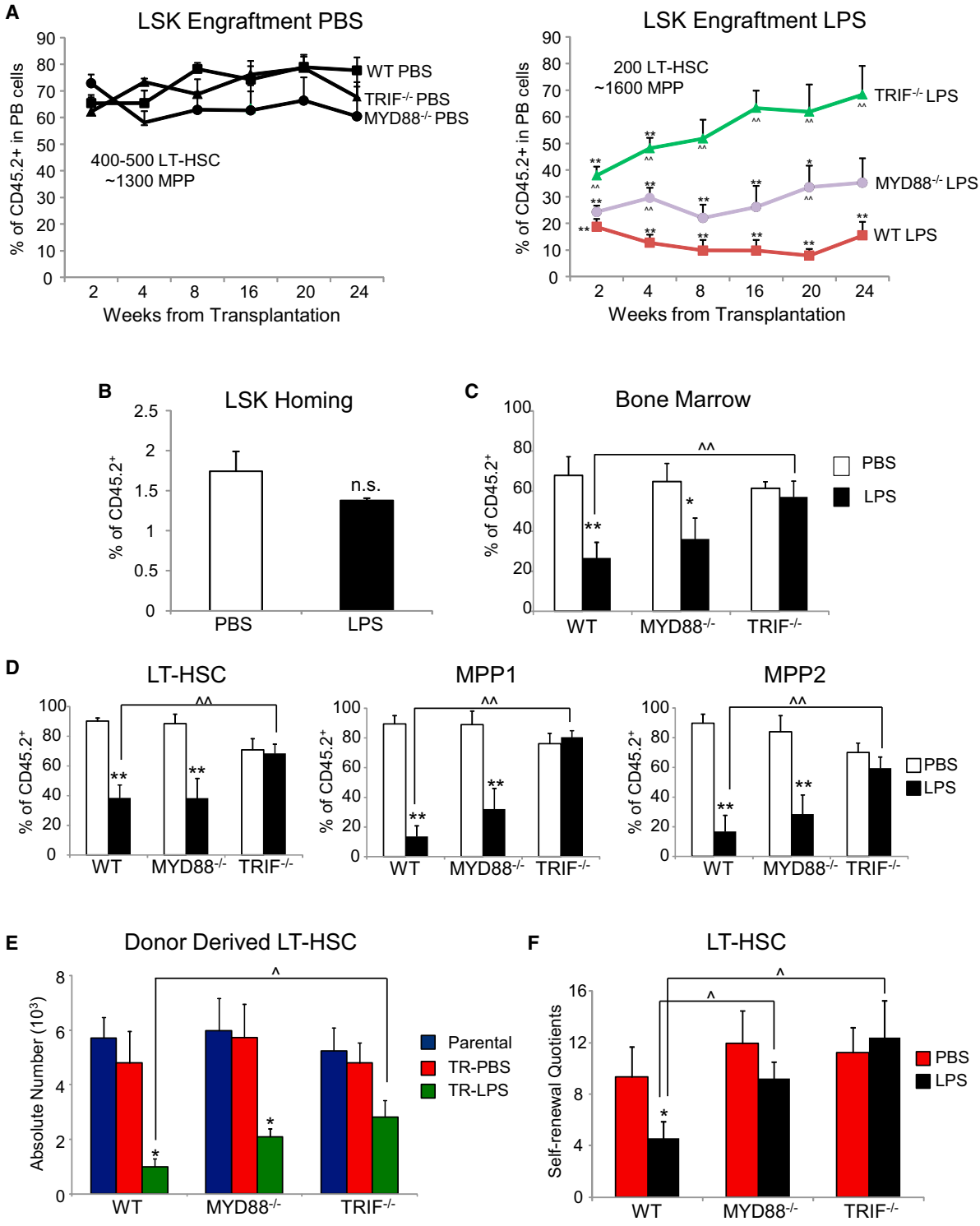

Figure 6. Loss of TRIF Preserves Long-Term Engraftment and Stem Cell Self-Renewal after Acute LPS Exposure

(A and C–E) 2,500 LSK cells sorted from PBS- or LPS-challenged WT, MYD88$^{-/-}$ and TRIF$^{-/-}$ mice (CD45.2^{+}) were transplanted into recipient BoyJ (CD45.1^{+}) and monitored for up to 24 weeks.

(A) Left: PBS LSK (400–500 LSKCD150^{+}CD48^{-}) donor cell engraftment (CD45.2^{+}) in the peripheral blood. n = 8–12. Right: LPS LSK (200 LSKCD150^{+}CD48^{-}) donor cell engraftment (CD45.2^{+}) in the peripheral blood. WT, n = 5–14; MyD88$^{-/-}$, n = 6–12; TRIF$^{-/-}$, n = 7–8.

(legend continued on next page)

significant increase when LT-HSC were defined as LSK FLK2^{-}CD34^{-}, likely for the greater inclusion of MPP. However, no changes were noticed when a more stringent LT-HSC definition was used (Oguro et al., 2013). We documented some contamination of the MPP pool by SCA-1-negative progenitors re-expressing SCA-1, as observed in HSC following pIpC (Pietras et al., 2014). However, this factor contributed only in part to the overall MPP expansion induced by LPS. In addition, surface expression of SCA-1 was not significantly increased in LT-HSC but was significantly upregulated in MPP. Thus, it is possible that primitive progenitors upregulate and prolong SCA-1 expression as part of the physiologic reaction to sepsis, as SCA-1 is also involved in maintaining HSPC function (Bradfute et al., 2005; Essers et al., 2009). The abnormal MPP expansion and SCA-1 upregulation induced by LPS was prevented by loss of TRIF, but not of MYD88, and the mixed chimera experiment showed that this effect is cell intrinsic.

Taken together, our data indicate that a balance between increased cell-cycle activation and increased apoptotic rates seems to account for maintenance of similar numbers of LT-HSC in LPS-treated mice and controls in all genotypes, although both processes were more intense in WT than in MYD88$^{-/-}$ or TRIF$^{-/-}$ mice. In contrast, differences in cell cycle, apoptosis, and progenitor cell contamination observed in the MPP pools do not sufficiently explain the significant MPP expansion in WT and MYD88$^{-/-}$ and the lack of it in TRIF$^{-/-}$ mice. It is possible that MPP commitment/differentiation is affected by LPS, and that a slow egression of MPP from the primitive to the differentiated cell pool (retention) also contributes to the expansion. As discussed later, this possibility is supported by the finding that critical transcription factors are altered in these cells and that they contribute poorly to short-term multilineage reconstitution after transplantation.

HSC functions are severely compromised following acute and chronic TLR4 activation (Esplin et al., 2011; Rodriguez et al., 2009). We demonstrated that TRIF signaling is a critical mediator of HSC injury, since its deletion fully restores HSC functions following LPS exposure. Transplantation of LPS LSK cells containing equal amounts of LT-HSC in WT, MYD88$^{-/-}$, and TRIF$^{-/-}$ mice revealed significant differences in long-term engraftment of these genotypes. WT LT-HSC from mice challenged with LPS were significantly exhausted at 24 weeks after transplant and showed low ability to self-renew and contribute to all lineages in competitive repopulation assays. In contrast, LPS TRIF$^{-/-}$ LT-HSC maintained their self-renewal and multilineage contribution, similarly to PBS controls. Loss of MYD88 provided some protection to HSC and progenitors, as LPS MYD88$^{-/-}$ LSK cells exhibited better engraftment than the LPS WT LSK cells, but did not fully rescue their functions. Interestingly, enrichment in MPP and contaminating progenitors in the LSK pool did not confer any advantage in short-term engraftment of WT and MYD88$^{-/-}$ LSK donor cells.

Collectively, our results show that HSC are qualitatively damaged by TRIF activation during LPS exposure and that this damage persists over the long term, and also in the presence of a healthy microenvironment. Strikingly, TRIF activation, unlike MYD88, did not directly cause myelosuppression. This cell-context-dependent effect does not seem to be mediated by differential expression of MYD88 or TRIF in the different subsets. Similar to the cell-context-dependent impact of other molecules (i.e., Notch), the distinct effects of TRIF and MYD88 are likely due to different requirements and molecular interactions of these two pathways in HSC and in myeloid progenitors. Potential mechanisms downstream of TRIF in HSC may involve STAT1, AKT, p38/ROS (Katsoulidis et al., 2005), or pathways activated by type I IFNs, which are known to damage HSC by induction of cell-cycle entry, apoptosis, and DNA damage (Baldridge et al., 2010; Pietras et al., 2014). However, mild induction of IFNs by LPS and lack of a protective effect in *Ifnra1*$^{-/-}$ mice following LPS suggest that this mechanism is not dominant in an LPS response.

Analysis of expression of *Spi1* and *CebpA*, two key transcription factors involved in the regulation of HSC and myeloid transcriptional programs (Hasemann et al.,

(B) Percentage of CD45.2^{+} cells in the BM of CD45.1^{+} BoyJ mice 16 hr after receiving 25,000 LSK cells sorted from LPS- or PBS-challenged WT (CD45.2^{+}) mice (n = 3).

(C) Percentage of donor engraftment of WT, MYD88$^{-/-}$, and TRIF$^{-/-}$ PBS or LPS LSK cells (CD45.2^{+}) in the BM of recipient mice at 24 weeks post transplantation (n = 7–9).

(D) Percentage of donor-derived CD45.2^{+} BM LT-HSC, MPP1, and MPP2 subsets in recipient mice (n = 7–9).

(E) Absolute number of donor-derived LT-HSC per femur: in WT, MYD88$^{-/-}$, and TRIF$^{-/-}$ mice at steady state, prior BM harvest for transplants (parental); at 24 weeks in transplanted recipients of sorted LSK cells from PBS-challenged mice (TR-PBS); and of sorted LSK cells from LPS-challenged mice (TR-LPS). n = 7–9.

(F) Self-renewal quotients of LT-HSC cells from PBS- and LPS-challenged WT, MYD88$^{-/-}$, and TRIF$^{-/-}$ mice at 24 weeks post transplantation. Quotient is calculated by dividing the absolute number of LT-HSC at 24 weeks by the average number of LT-HSC input at the time of transplantation. n = 7–9.

Data were from two independent experiments and represent mean ± SEM. LPS versus PBS: *p < 0.05, **p < 0.01; WT versus MYD88$^{-/-}$ or TRIF$^{-/-}$: ^p < 0.05, ^^p < 0.01. n.s., not significant.

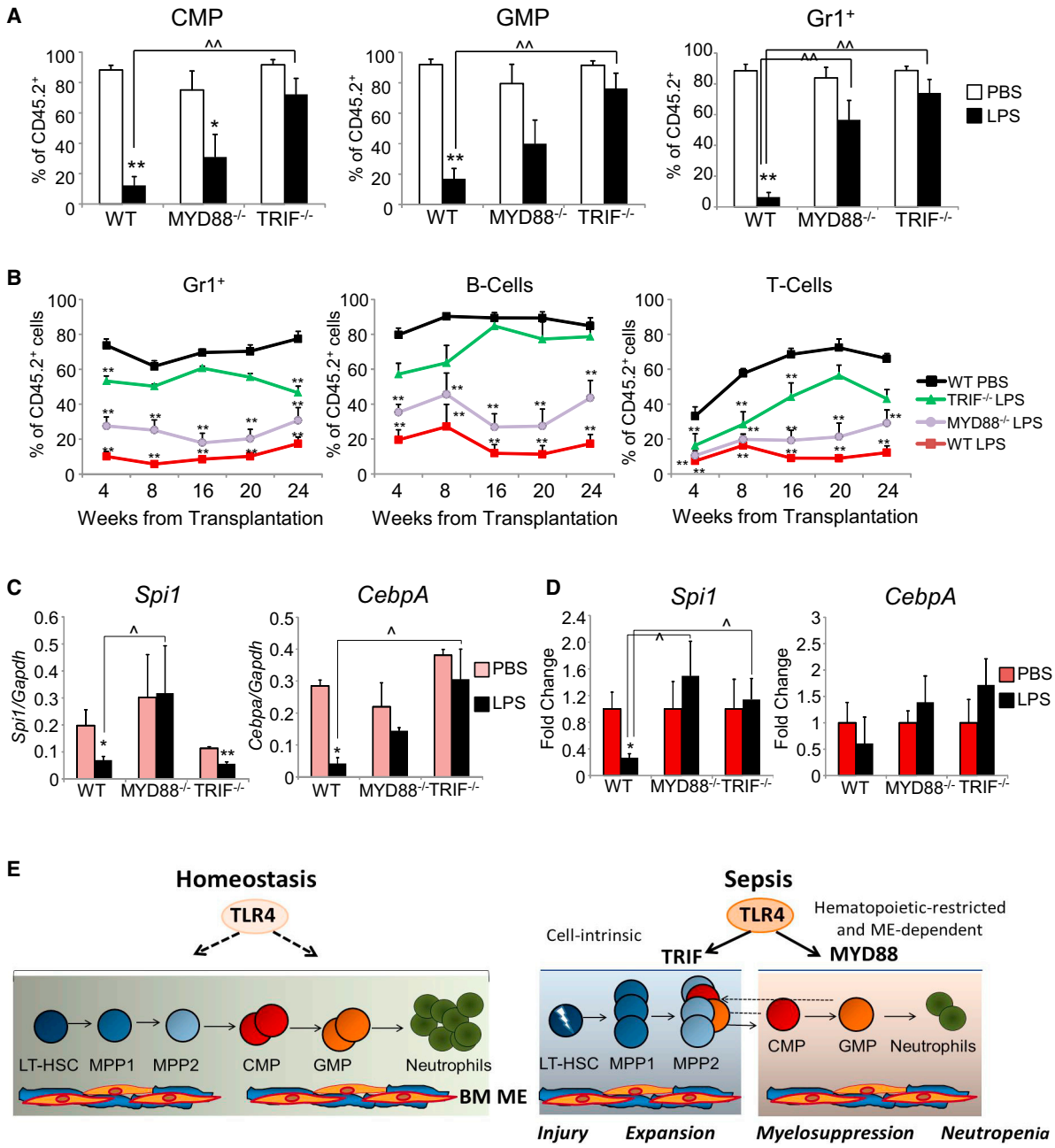

Figure 7. Impact of LPS on Multilineage Reconstitution and on of PU.1 and CEBP/α

(A and B) 2,500 LSK cells sorted from PBS- or LPS-challenged WT, MYD88$^{-/-}$, and TRIF$^{-/-}$ mice (CD45.2^{+}) were transplanted into recipient BoyJ (CD45.1^{+}). Recipients were monitored for up to 24 weeks.

(A) Percentage of donor-derived CD45.2^{+} BM CMP (left), GMP (middle), and GR1^{+} (right) in recipient mice at week 24 (n = 7–9).

(B) Line graphs show mean percentage of donor CD45.2^{+} cells in in myeloid cells (GR1^{+}), B cells (B220^{+}), and T cells (CD4^{+} or CD8^{+}) in peripheral blood of recipient mice after transplantation (n = 7–16).

(C) Relative mRNA expression level of *Spi1* and *CebpA* in LSK cells sorted from WT (n = 5–9 samples), MYD88$^{-/-}$ (n = 4–5 samples), and TRIF$^{-/-}$ (n = 3 samples) mice challenged with PBS or LPS for 24 hr; each sample derived from cells pooled from 2–3 mice; minimum of three independent experiments.

(D) WT, MYD88$^{-/-}$, and TRIF$^{-/-}$ LSK cells were sorted at 24 weeks after transplantation. Fold change of expression level of *Spi1* and *CebpA* (n = 3–4 samples derived from cells pooled from 2–3 mice).

(legend continued on next page)

2014; Staber et al., 2013), revealed that they were significantly downregulated in WT HSPC following LPS treatment, while their levels were preserved in the absence of MYD88 (*Spi1*) or TRIF (*CebpA*). *Spi1* and *CebpA* expression levels continued to remain low in HSCs at 24 weeks following transplant, whereas they were restored in MYD88$^{-/-}$ and TRIF$^{-/-}$ HSPC. Thus, our study shows that acute exposure of HSPC to LPS endotoxemia is sufficient to induce permanent transcriptional changes even when the endotoxic environment is removed and cells are transplanted in healthy donors. Changes in histone methylation patterns in mature cells have been reported following sepsis (Carson et al., 2011), and we found changes in epigenetic modifications in HSPC after in vivo exposure to LPS (H.Z. and N.C., unpublished observations). Further studies are necessary to address the impact of epigenetic regulation of HSC on their function and differentiation during sepsis.

In conclusion, the present study shows that TRIF and MYD88 uncouple effects of TLR4 signaling on HSC and myeloid progenitors during severe bacterial infection. This observation has potential clinical relevance. Despite the central role for TLR4 in sepsis, a recent randomized clinical trial failed to show survival improvement in patients with sepsis treated with a TLR4 antagonist (Opal et al., 2013). It is likely that complete inhibition of TLR4 signaling, with simultaneous inhibition of the MYD88 and TRIF pathway, also abrogates its protective effects, thus compromising the effectiveness of this therapeutic approach. The results presented here provide a guide to further dissect the independent effects of MYD88 and TRIF during response to severe bacterial infection and support the rationale for pursuing time-tuned selective silencing of one pathway (MYD88 or TRIF) to mitigate myelosuppression or stem cell injury. Finally, these observations may also provide insight into the impact of MYD88 and TRIF in HSC and myeloid progenitors during chronic inflammation related to aging and hematopoietic cell malignant transformation.

EXPERIMENTAL PROCEDURES

See Supplemental Experimental Procedures for details on mice, flow cytometry and cell sorting, cell-cycle and apoptosis analysis, myeloid progenitor and Lys-GFP in vitro differentiation assay, and gene expression.

Endotoxemia and Sepsis Models

All animal experiments were approved by the Institutional Animal Care and Use Committee of the Indiana University School of Medicine (IUSM). Mice were subjected to intraperitoneal inoculation of 3 mg/kg *P. aeruginosa* LPS (Rodriguez et al., 2009) purchased from Sigma-Aldrich (L8643) and were analyzed 24 hr after challenge. Severe sepsis was induced by CLP using a 21G1 1/2-gauge needle, as described by Ferreira et al. (2014). Sham mice received cecal ligation but no perforation of the cecum. Mice were euthanized 24 hr after the CLP surgery for BM analysis.

Generation of Chimeras

WT/MYD88$^{-/-}$ or WT/TRIF$^{-/-}$ chimeras were generated by transplantation via tail-vein injection of 2 × 10^6 BM cells from BoyJ (CD45.1$^+$) mice into lethally irradiated MYD88$^{-/-}$ or TRIF$^{-/-}$ (CD45.2$^+$) recipients. MYD88$^{-/-}$/WT or TRIF$^{-/-}$/WT chimeras were generated by transplantation via tail-vein injection of 2 × 10^6 BM cells from MYD88$^{-/-}$ or TRIF$^{-/-}$ (CD45.2$^+$) mice into lethally irradiated BoyJ (CD45.1$^+$) recipients. Mixed chimeras were generated by using WT cells from the Ubi-GFP mouse (CD45.2$^+$) as follows. WT, MYD88$^{-/-}$, or TRIF$^{-/-}$ BM cells (CD45.2$^+$; 1 × 10^6 cells) were mixed 1:1 with WT-GFP$^+$ (CD45.2$^+$) BM cells and transplanted into lethally irradiated BoyJ (CD45.1$^+$) recipients. Engraftment >80% was confirmed in the peripheral blood 8–10 weeks after transplantation when chimeras were challenged with LPS or PBS.

Competitive Repopulation Assay

A total of 2,500 LSK donor cells from PBS- or LPS-challenged WT, MYD88$^{-/-}$, and TRIF$^{-/-}$ mice (CD45.2$^+$) were sorted and transplanted into lethally irradiated BoyJ mice (CD45.1$^+$). A dose of 10^5 CD45.1$^+$ BM cells were used as competitors. Engraftment was evaluated in the peripheral blood at 4-week intervals until week 24. At week 24, all recipients were euthanized for BM analysis.

Statistical Analysis

Equality of distributions for matched pairs of observations was tested with Student's t test. Comparisons were made of LPS versus PBS and KO versus WT using unpaired t test and ANOVA when appropriate. Significance in figures is indicated by *$p < 0.05$ or ^$p < 0.05$ and **$p < 0.01$ or ^^$p < 0.01$. Measurements were performed in at least three independent

(E) Working model. TRIF and MYD88 uncouple the effects of TLR4-mediated injury on hematopoietic stem cells and myeloid progenitors during severe sepsis. The role of TLR4 in regulating hematopoiesis in homeostatic conditions is still unclear. It is possible that the gut microbiota maintains a systemic basal state of TLR4 activation. In the state of severe sepsis, maximal activation of TLR4 by bacterial LPS activates: (1) TRIF, leading to injury of LT-HSC (Figure 6) and dysfunctional expansion of MPPs by cell-cycle activation, shift of progenitors re-expressing SCA-1, and impaired egress (Figures 1E, 1F, 2, 7A, and 7B); and (2) MYD88, resulting in damage of myeloid progenitors by increased apoptosis and impaired differentiation (Figures 3 and 5). Cell-autonomous and non-cell-autonomous mechanisms contribute to these effects in both pathways (Figure 4).
Data represent mean ± SEM. LPS versus PBS: *$p < 0.05$, **$p < 0.01$; WT versus MYD88$^{-/-}$ or TRIF$^{-/-}$: ^$p < 0.05$, ^^$p < 0.01$.

experiments. N indicates the number of individual mice used unless noted otherwise.

SUPPLEMENTAL INFORMATION

Supplemental Information includes Supplemental Experimental Procedures, seven figures, and two tables and can be found with this article online at http://dx.doi.org/10.1016/j.stemcr.2016.05.002.

AUTHOR CONTRIBUTIONS

H.Z. performed all the experiments and wrote the manuscript. S.R. assisted with transplantation models. L.W. assisted with chimeras. S.W. performed CLP modeling. H.S. designed and supervised CLP experiments. R.K. and A.A.C. contributed intellectually. N.C. designed the experiments and wrote the manuscript.

ACKNOWLEDGMENTS

The authors thank the NIH R01 HL068256-05 and R01 DK097837-09 (N.C.), the MPN Research Foundation (N.C.), the Showalter Grant (N.C.), the AHA (H.Z.), the NIDDK CEMH (N.C. and A.A.C.), and R01 HL124159-01 (H.S.). The authors thank IUSM In Vivo Therapeutics Core and the Flow Cytometry Resource Facility.

Received: May 1, 2015
Revised: May 6, 2016
Accepted: May 8, 2016
Published: June 2, 2016

REFERENCES

Angus, D.C. (2011). The search for effective therapy for sepsis: back to the drawing board? JAMA *306*, 2614–2615.

Baldridge, M.T., King, K.Y., Boles, N.C., Weksberg, D.C., and Goodell, M.A. (2010). Quiescent haematopoietic stem cells are activated by IFN-gamma in response to chronic infection. Nature *465*, 793–797.

Beutler, B. (2000). Tlr4: central component of the sole mammalian LPS sensor. Curr. Opin. Immunol. *12*, 20–26.

Boettcher, S., Gerosa, R.C., Radpour, R., Bauer, J., Ampenberger, F., Heikenwalder, M., Kopf, M., and Manz, M.G. (2014). Endothelial cells translate pathogen signals into G-CSF-driven emergency granulopoiesis. Blood *124*, 1393–1403.

Bosmann, M., and Ward, P.A. (2013). The inflammatory response in sepsis. Trends Immunol. *34*, 129–136.

Bradfute, S.B., Graubert, T.A., and Goodell, M.A. (2005). Roles of Sca-1 in hematopoietic stem/progenitor cell function. Exp. Hematol. *33*, 836–843.

Carson, W.F., Cavassani, K.A., Dou, Y., and Kunkel, S.L. (2011). Epigenetic regulation of immune cell functions during post-septic immunosuppression. Epigenetics *6*, 273–283.

Challen, G.A., Sun, D., Jeong, M., Luo, M., Jelinek, J., Berg, J.S., Bock, C., Vasanthakumar, A., Gu, H., Xi, Y., et al. (2012). Dnmt3a is essential for hematopoietic stem cell differentiation. Nat. Genet. *44*, 23–31.

Esplin, B.L., Shimazu, T., Welner, R.S., Garrett, K.P., Nie, L., Zhang, Q., Humphrey, M.B., Yang, Q., Borghesi, L.A., and Kincade, P.W. (2011). Chronic exposure to a TLR ligand injures hematopoietic stem cells. J. Immunol. *186*, 5367–5375.

Essers, M.A., Offner, S., Blanco-Bose, W.E., Waibler, Z., Kalinke, U., Duchosal, M.A., and Trumpp, A. (2009). IFNalpha activates dormant haematopoietic stem cells in vivo. Nature *458*, 904–908.

Faust, N., Varas, F., Kelly, L.M., Heck, S., and Graf, T. (2000). Insertion of enhanced green fluorescent protein into the lysozyme gene creates mice with green fluorescent granulocytes and macrophages. Blood *96*, 719–726.

Ferreira, A.E., Sisti, F., Sonego, F., Wang, S., Filgueiras, L.R., Brandt, S., Serezani, A.P., Du, H., Cunha, F.Q., Alves-Filho, J.C., et al. (2014). PPAR-gamma/IL-10 axis inhibits MyD88 expression and ameliorates murine polymicrobial sepsis. J. Immunol. *192*, 2357–2365.

Hasemann, M.S., Lauridsen, F.K., Waage, J., Jakobsen, J.S., Frank, A.K., Schuster, M.B., Rapin, N., Bagger, F.O., Hoppe, P.S., Schroeder, T., et al. (2014). C/EBPalpha is required for long-term self-renewal and lineage priming of hematopoietic stem cells and for the maintenance of epigenetic configurations in multipotent progenitors. PLoS Genet. *10*, e1004079.

Hotchkiss, R.S., and Karl, I.E. (2003). The pathophysiology and treatment of sepsis. N. Engl. J. Med. *348*, 138–150.

Katsoulidis, E., Li, Y., Mears, H., and Platanias, L.C. (2005). The p38 mitogen-activated protein kinase pathway in interferon signal transduction. J. Interferon Cytokine Res. *25*, 749–756.

Kawai, T., Takeuchi, O., Fujita, T., Inoue, J., Muhlradt, P.F., Sato, S., Hoshino, K., and Akira, S. (2001). Lipopolysaccharide stimulates the MyD88-independent pathway and results in activation of IFN-regulatory factor 3 and the expression of a subset of lipopolysaccharide-inducible genes. J. Immunol. *167*, 5887–5894.

Kiel, M.J., Yilmaz, O.H., Iwashita, T., Terhorst, C., and Morrison, S.J. (2005). SLAM family receptors distinguish hematopoietic stem and progenitor cells and reveal endothelial niches for stem cells. Cell *121*, 1109–1121.

Miyamoto, T., Iwasaki, H., Reizis, B., Ye, M., Graf, T., Weissman, I.L., and Akashi, K. (2002). Myeloid or lymphoid promiscuity as a critical step in hematopoietic lineage commitment. Dev. Cell *3*, 137–147.

Nagai, Y., Garrett, K.P., Ohta, S., Bahrun, U., Kouro, T., Akira, S., Takatsu, K., and Kincade, P.W. (2006). Toll-like receptors on hematopoietic progenitor cells stimulate innate immune system replenishment. Immunity *24*, 801–812.

Oguro, H., Ding, L., and Morrison, S.J. (2013). SLAM family markers resolve functionally distinct subpopulations of hematopoietic stem cells and multipotent progenitors. Cell Stem Cell *13*, 102–116.

O'Neill, L.A., and Bowie, A.G. (2007). The family of five: TIR-domain-containing adaptors in Toll-like receptor signalling. Nat. Rev. Immunol. *7*, 353–364.

Opal, S.M., Laterre, P.F., Francois, B., LaRosa, S.P., Angus, D.C., Mira, J.P., Wittebole, X., Dugernier, T., Perrotin, D., Tidswell, M., et al. (2013). Effect of eritoran, an antagonist of MD2-TLR4, on mortality in patients with severe sepsis: the ACCESS randomized trial. JAMA *309*, 1154–1162.

Pietras, E.M., Lakshminarasimhan, R., Techner, J.M., Fong, S., Flach, J., Binnewies, M., and Passegue, E. (2014). Re-entry into quiescence protects hematopoietic stem cells from the killing effect of chronic exposure to type I interferons. J. Exp. Med. *211*, 245–262.

Poltorak, A., He, X., Smirnova, I., Liu, M.Y., Van Huffel, C., Du, X., Birdwell, D., Alejos, E., Silva, M., Galanos, C., et al. (1998). Defective LPS signaling in C3H/HeJ and C57BL/10ScCr mice: mutations in Tlr4 gene. Science *282*, 2085–2088.

Rodriguez, S., Chora, A., Goumnerov, B., Mumaw, C., Goebel, W.S., Fernandez, L., Baydoun, H., HogenEsch, H., Dombkowski, D.M., Karlewicz, C.A., et al. (2009). Dysfunctional expansion of hematopoietic stem cells and block of myeloid differentiation in lethal sepsis. Blood *114*, 4064–4076.

Roger, T., Froidevaux, C., Le Roy, D., Reymond, M.K., Chanson, A.L., Mauri, D., Burns, K., Riederer, B.M., Akira, S., and Calandra, T. (2009). Protection from lethal gram-negative bacterial sepsis by targeting Toll-like receptor 4. Proc. Natl. Acad. Sci. USA *106*, 2348–2352.

Staber, P.B., Zhang, P., Ye, M., Welner, R.S., Nombela-Arrieta, C., Bach, C., Kerenyi, M., Bartholdy, B.A., Zhang, H., Alberich-Jorda, M., et al. (2013). Sustained PU.1 levels balance cell-cycle regulators to prevent exhaustion of adult hematopoietic stem cells. Mol. Cell *49*, 934–946.

van Lieshout, M.H., Blok, D.C., Wieland, C.W., de Vos, A.F., van 't Veer, C., and van der Poll, T. (2012). Differential roles of MyD88 and TRIF in hematopoietic and resident cells during murine gram-negative pneumonia. J. Infect. Dis. *206*, 1415–1423.

Vincent, J.L., Rello, J., Marshall, J., Silva, E., Anzueto, A., Martin, C.D., Moreno, R., Lipman, J., Gomersall, C., Sakr, Y., et al. (2009). International study of the prevalence and outcomes of infection in intensive care units. JAMA *302*, 2323–2329.

Weighardt, H., and Holzmann, B. (2007). Role of Toll-like receptor responses for sepsis pathogenesis. Immunobiology *212*, 715–722.

Weighardt, H., Kaiser-Moore, S., Vabulas, R.M., Kirschning, C.J., Wagner, H., and Holzmann, B. (2002). Cutting edge: myeloid differentiation factor 88 deficiency improves resistance against sepsis caused by polymicrobial infection. J. Immunol. *169*, 2823–2827.

Weighardt, H., Jusek, G., Mages, J., Lang, R., Hoebe, K., Beutler, B., and Holzmann, B. (2004). Identification of a TLR4- and TRIF-dependent activation program of dendritic cells. Eur. J. Immunol. *34*, 558–564.

Wilson, A., Laurenti, E., Oser, G., van der Wath, R.C., Blanco-Bose, W., Jaworski, M., Offner, S., Dunant, C.F., Eshkind, L., Bockamp, E., et al. (2008). Hematopoietic stem cells reversibly switch from dormancy to self-renewal during homeostasis and repair. Cell *135*, 1118–1129.

Yamamoto, M., Sato, S., Hemmi, H., Hoshino, K., Kaisho, T., Sanjo, H., Takeuchi, O., Sugiyama, M., Okabe, M., Takeda, K., et al. (2003). Role of adaptor TRIF in the MyD88-independent toll-like receptor signaling pathway. Science *301*, 640–643.

Stem Cell Reports, Volume *6*

Supplemental Information

Sepsis Induces Hematopoietic Stem Cell Exhaustion and Myelosuppression through Distinct Contributions of TRIF and MYD88

Huajia Zhang, Sonia Rodriguez, Lin Wang, Soujuan Wang, Henrique Serezani, Reuben Kapur, Angelo A. Cardoso, and Nadia Carlesso

Figure S1

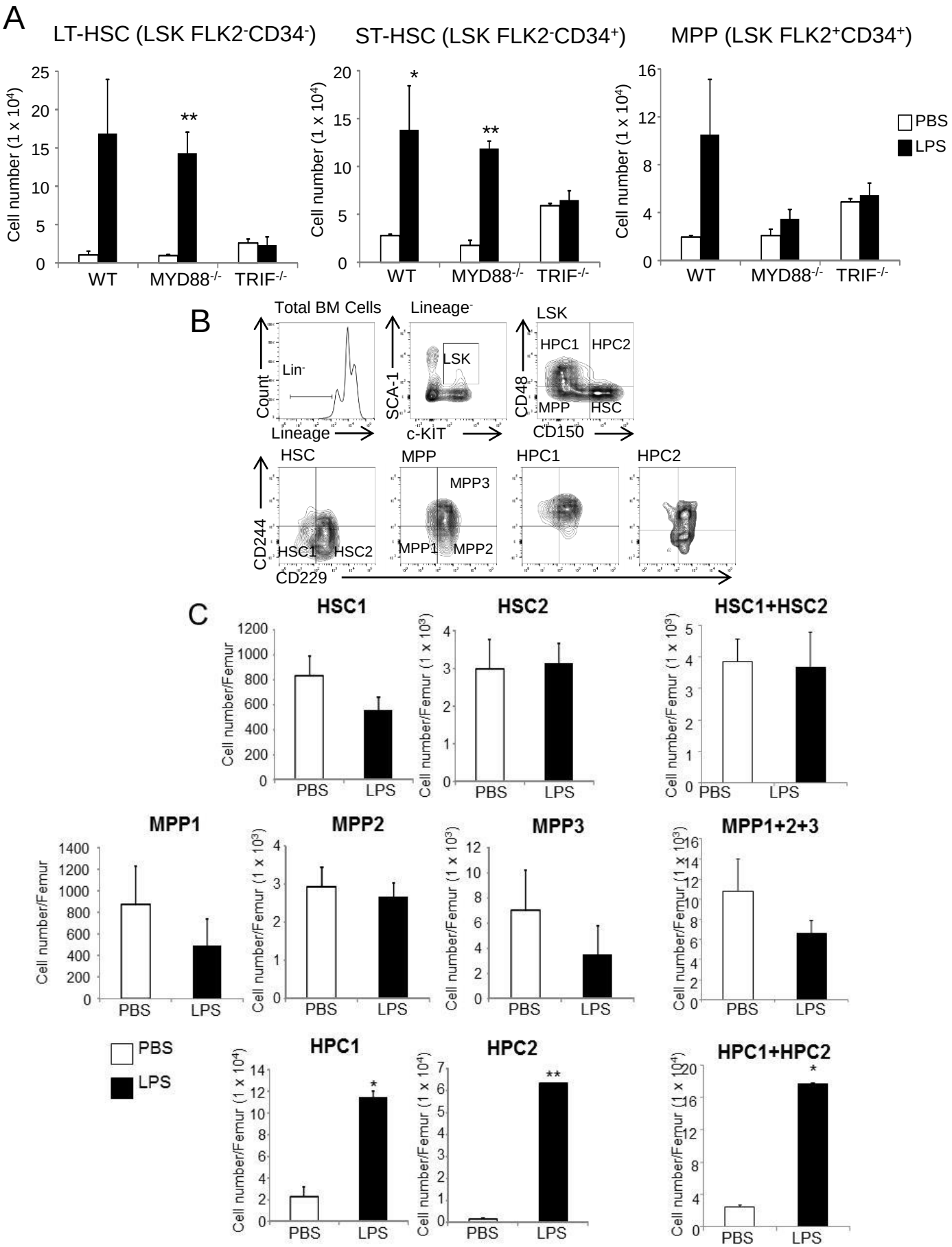
A
LT-HSC (LSK FLK2-CD34-)
ST-HSC (LSK FLK2-CD34+)
MPP (LSK FLK2+CD34+)
Cell number (1 x 10^4)
WT
MYD88-/-
TRIF-/-
PBS
LPS
B
Total BM Cells
Lineage-
LSK
Lin-
Count
Lineage
SCA-1
c-KIT
LSK
CD48
CD150
HPC1
HPC2
MPP
HSC
CD244
CD229
HSC1
HSC2
MPP1
MPP2
MPP3
C
HSC1
HSC2
HSC1+HSC2
MPP1
MPP2
MPP3
MPP1+2+3
HPC1
HPC2
HPC1+HPC2
Cell number/Femur
Cell number/Femur (1 x 10^3)
Cell number/Femur (1 x 10^4)

Figure S2

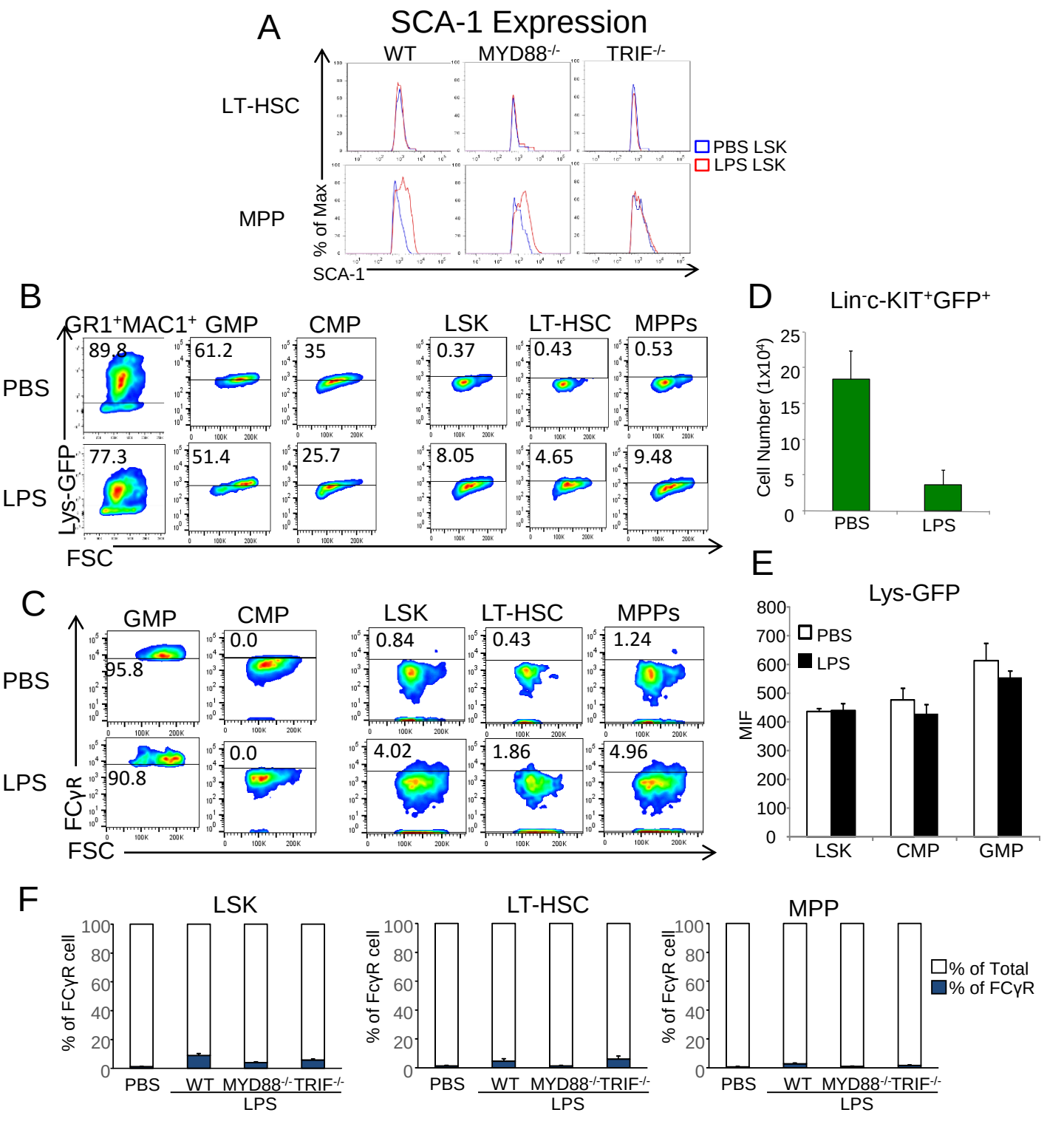
A
SCA-1 Expression
WT
MYD88-/-
TRIF-/-
LT-HSC
MPP
% of Max
SCA-1
PBS LSK
LPS LSK
B
GR1+MAC1+ GMP
CMP
LSK
LT-HSC
MPPs
PBS
LPS
Lys-GFP
FSC
89.8
61.2
35
0.37
0.43
0.53
77.3
51.4
25.7
8.05
4.65
9.48
C
GMP
CMP
LSK
LT-HSC
MPPs
PBS
LPS
FCγR
FSC
95.8
0.0
0.84
0.43
1.24
90.8
0.0
4.02
1.86
4.96
D
Lin-c-KIT+GFP+
Cell Number (1x10^4)
PBS
LPS
E
Lys-GFP
MIF
PBS
LPS
LSK
CMP
GMP
F
LSK
LT-HSC
MPP
% of FCγR cell
PBS
WT
MYD88-/-
TRIF-/-
LPS
% of Total
% of FCγR

Figure S3

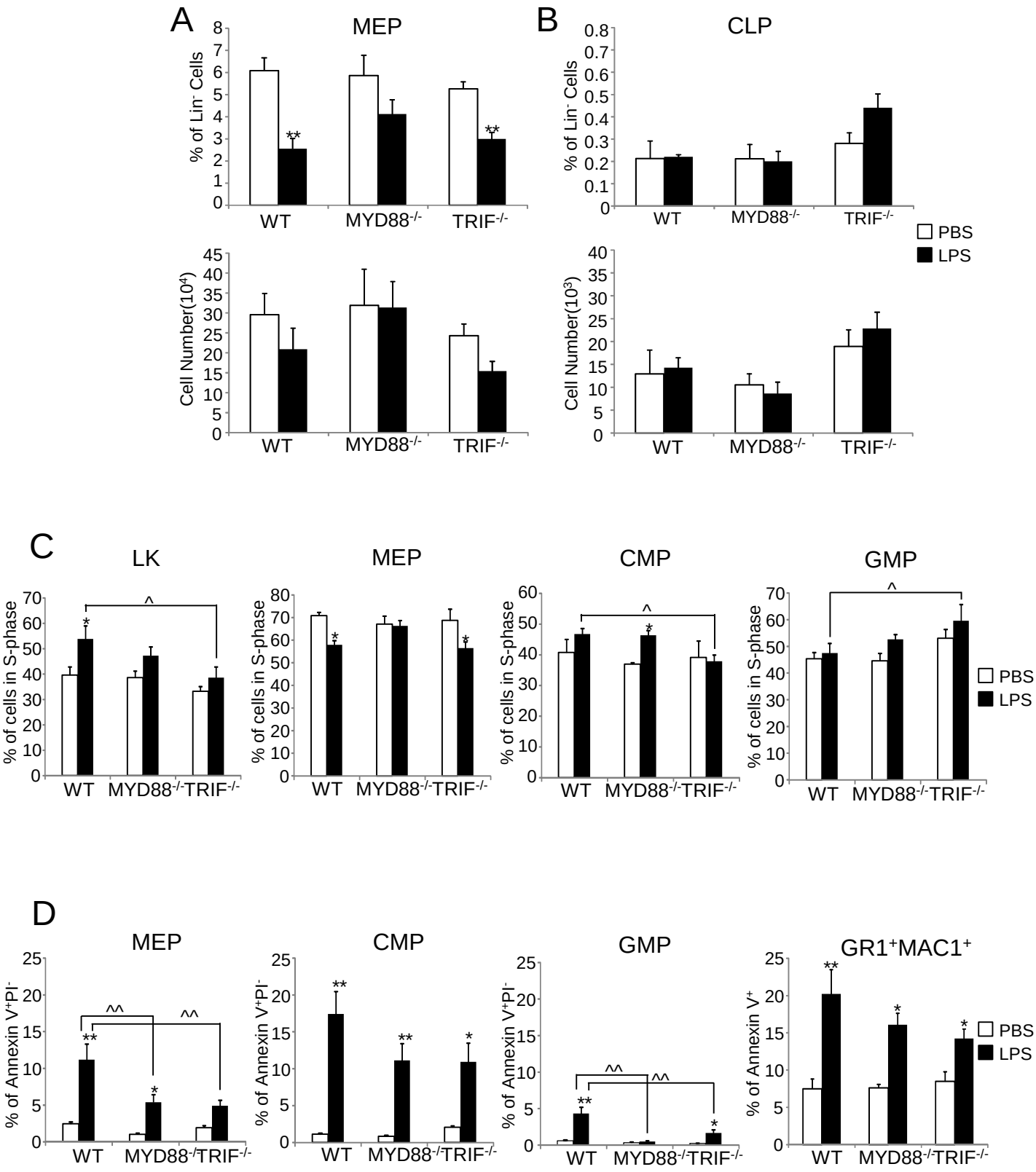
A
MEP
% of Lin- Cells
Cell Number(10^4)
WT
MYD88-/-
TRIF-/-
B
CLP
% of Lin- Cells
Cell Number(10^3)
PBS
LPS
C
LK
MEP
CMP
GMP
% of cells in S-phase
WT
MYD88-/-TRIF-/-
D
MEP
CMP
GMP
GR1+MAC1+
% of Annexin V+PI-
% of Annexin V+

Figure S4

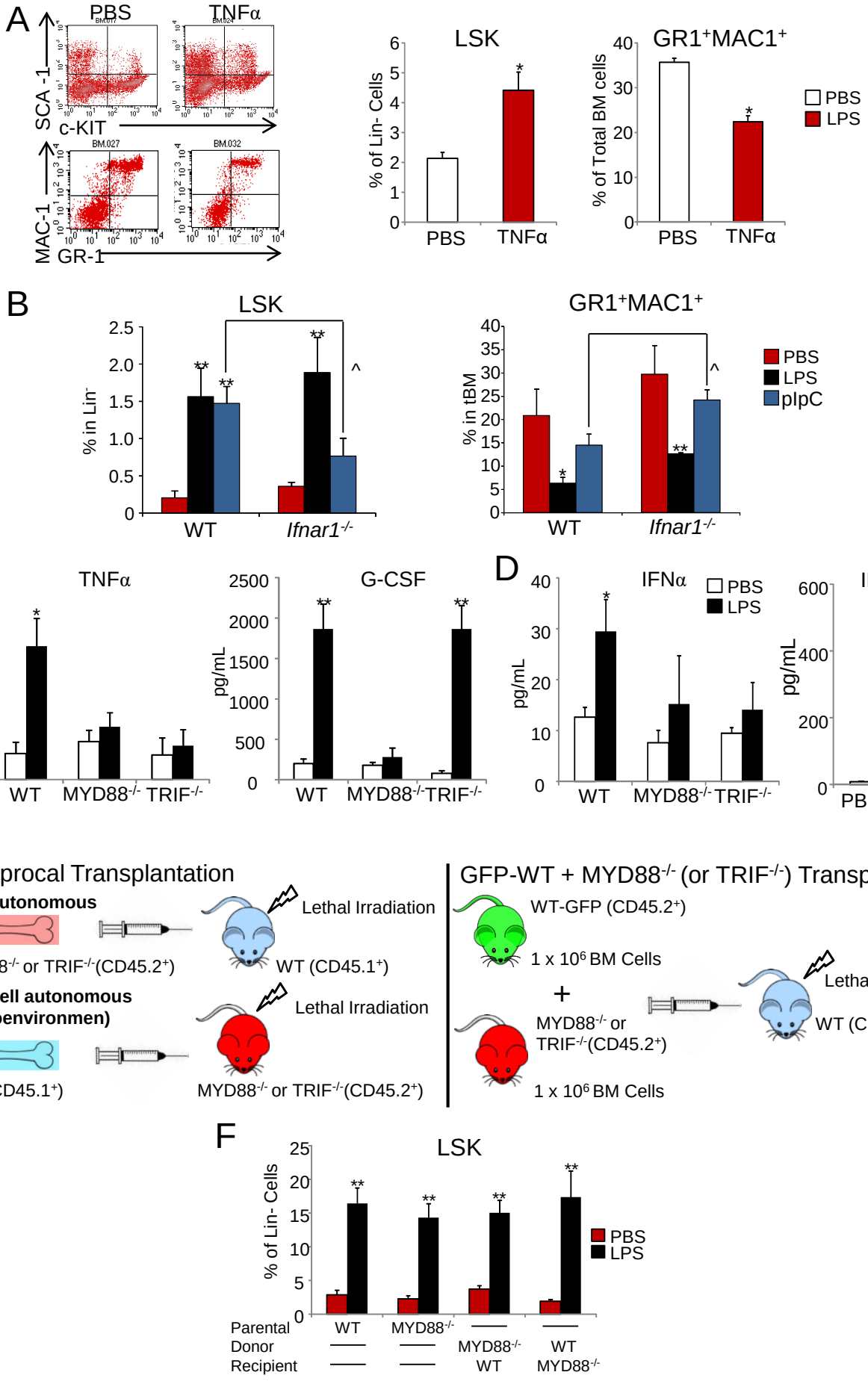
A
PBS
TNFα
SCA -1
c-KIT
MAC-1
GR-1
LSK
% of Lin- Cells
GR1+MAC1+
% of Total BM cells
PBS
LPS
B
LSK
% in Lin-
GR1+MAC1+
% in tBM
PBS
LPS
pIpC
WT
Ifnar1-/-
C
TNFα
G-CSF
pg/mL
WT
MYD88-/-
TRIF-/-
D
IFNα
pg/mL
PBS
pIpC
E
Reciprocal Transplantation
Cell Autonomous
MYD88-/- or TRIF-/-(CD45.2+)
Lethal Irradiation
WT (CD45.1+)
Non-cell autonomous (Microenvironmen)
WT (CD45.1+)
Lethal Irradiation
MYD88-/- or TRIF-/-(CD45.2+)
GFP-WT + MYD88-/- (or TRIF-/-) Transplantation
WT-GFP (CD45.2+)
1 x 10^6 BM Cells
+
MYD88-/- or TRIF-/-(CD45.2+)
1 x 10^6 BM Cells
Lethal Irradiation
WT (CD45.1+)
F
LSK
% of Lin- Cells
PBS
LPS
Parental
Donor
Recipient
WT
MYD88-/-
MYD88-/-
WT
WT
MYD88-/-

Figure S5

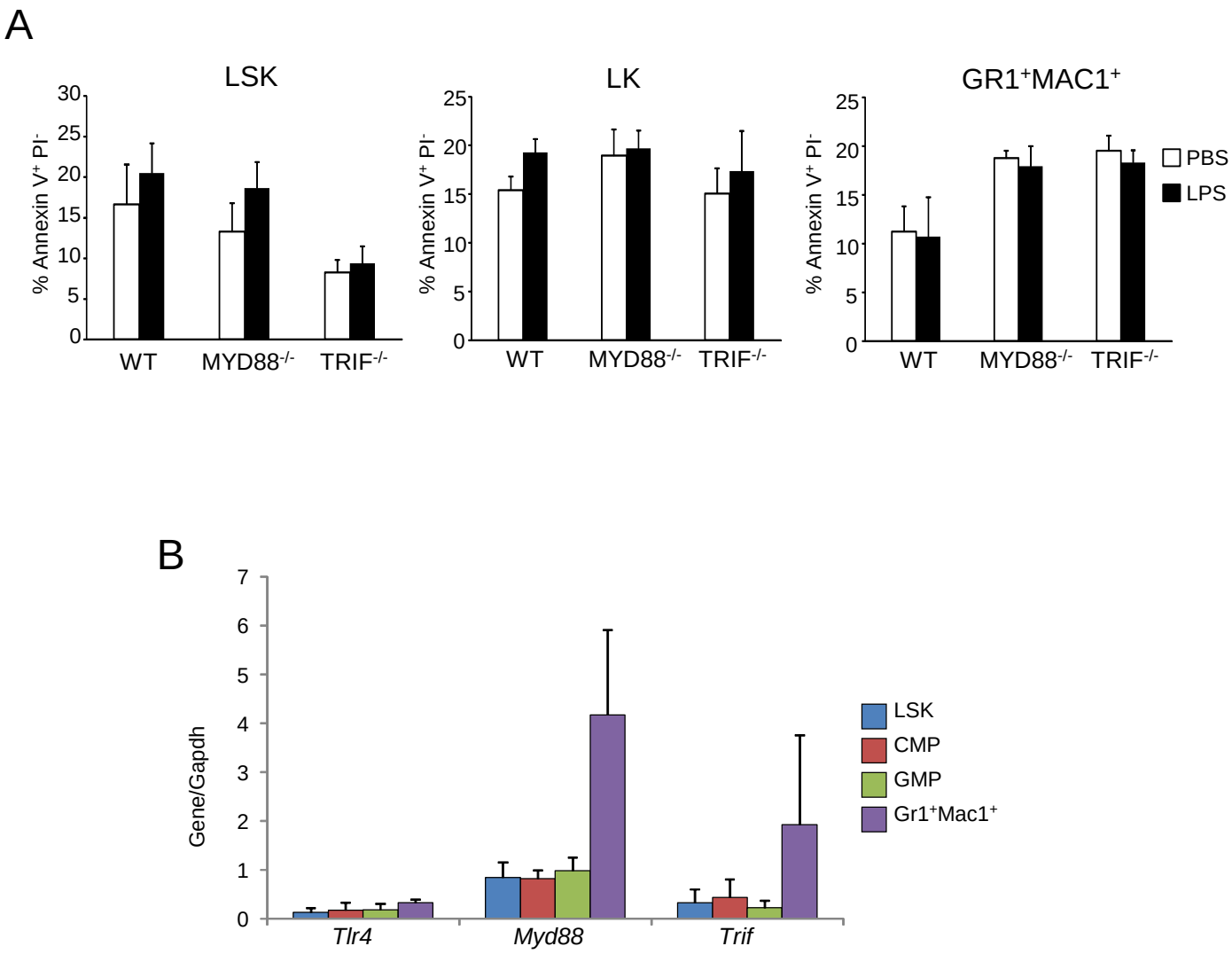
A
LSK
LK
GR1+MAC1+
% Annexin V+ PI-
30
25
20
15
10
5
0
WT
MYD88-/-
TRIF-/-
PBS
LPS
B
Gene/Gapdh
7
6
5
4
3
2
1
0
Tlr4
Myd88
Trif
LSK
CMP
GMP
Gr1+Mac1+

Figure S6

A

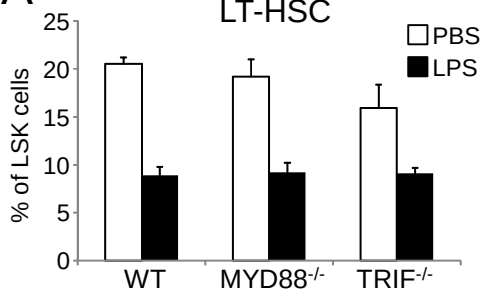

% of LT-HSC in LSK cells				Cell/2500 LSK		LT-HSC adjusted		
	PBS	SEM	LPS	SEM	PBS	LPS	PBS	LPS
WT	20.5	±0.66	8.87	±0.91	512	211	512	200.872
MYD88$^{-/-}$	19.1	±1.79	9.19	±0.97	478	229	467.484	225.794
TRIF$^{-/-}$	15.9	±2.46	9.09	±0.57	397	227	392.236	211.564

B

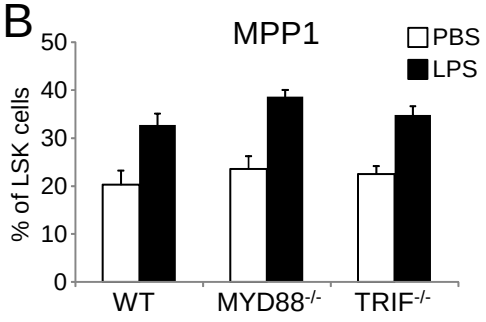

% of MPP1 in LSK cells				Cells/2500 cells		MPP1 adjusted		
	PBS	SEM	LPS	SEM	PBS	LPS	PBS	LPS
WT	20.2	±2.97	32.7	±2.42	505	817	498.94	794.941
MYD88$^{-/-}$	23.6	±2.62	38.6	±1.43	590	965	587.64	955.35
TRIF$^{-/-}$	22.6	±1.86	34.7	±1.84	565	867	559.915	852.261

C

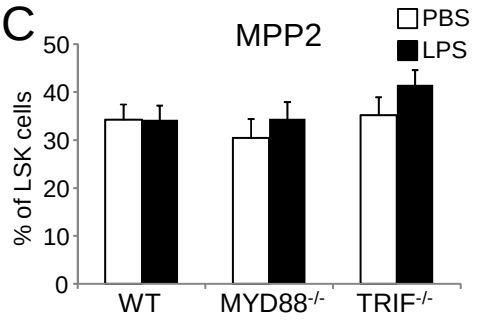

% of MPP2 in LSK cells				Cells/2500 cells		MPP2 adjusted		
	PBS	SEM	LPS	SEM	PBS	LPS	PBS	LPS
WT	34.2	±3.17	34.2	±2.9	856	855	845.728	831.915
MYD88$^{-/-}$	30.4	±3.98	34.4	±3.49	761	861	757.956	852.39
TRIF$^{-/-}$	33	±3.33	41.5	±3.10	826	1038	818.566	1020.354

D

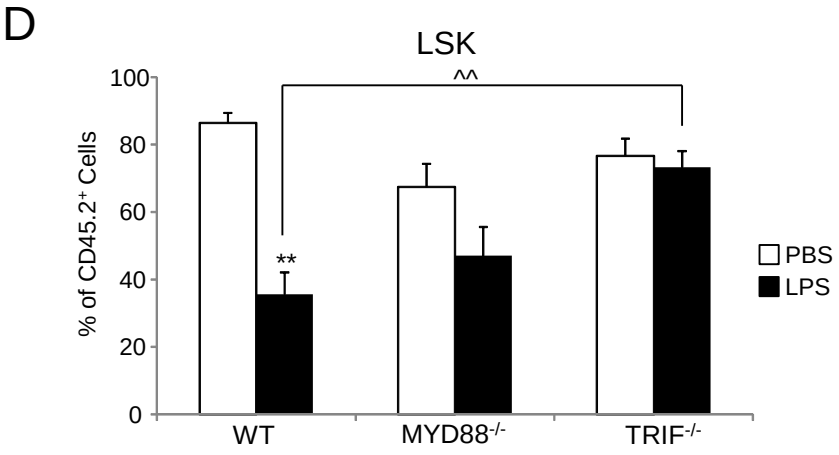

Figure S7

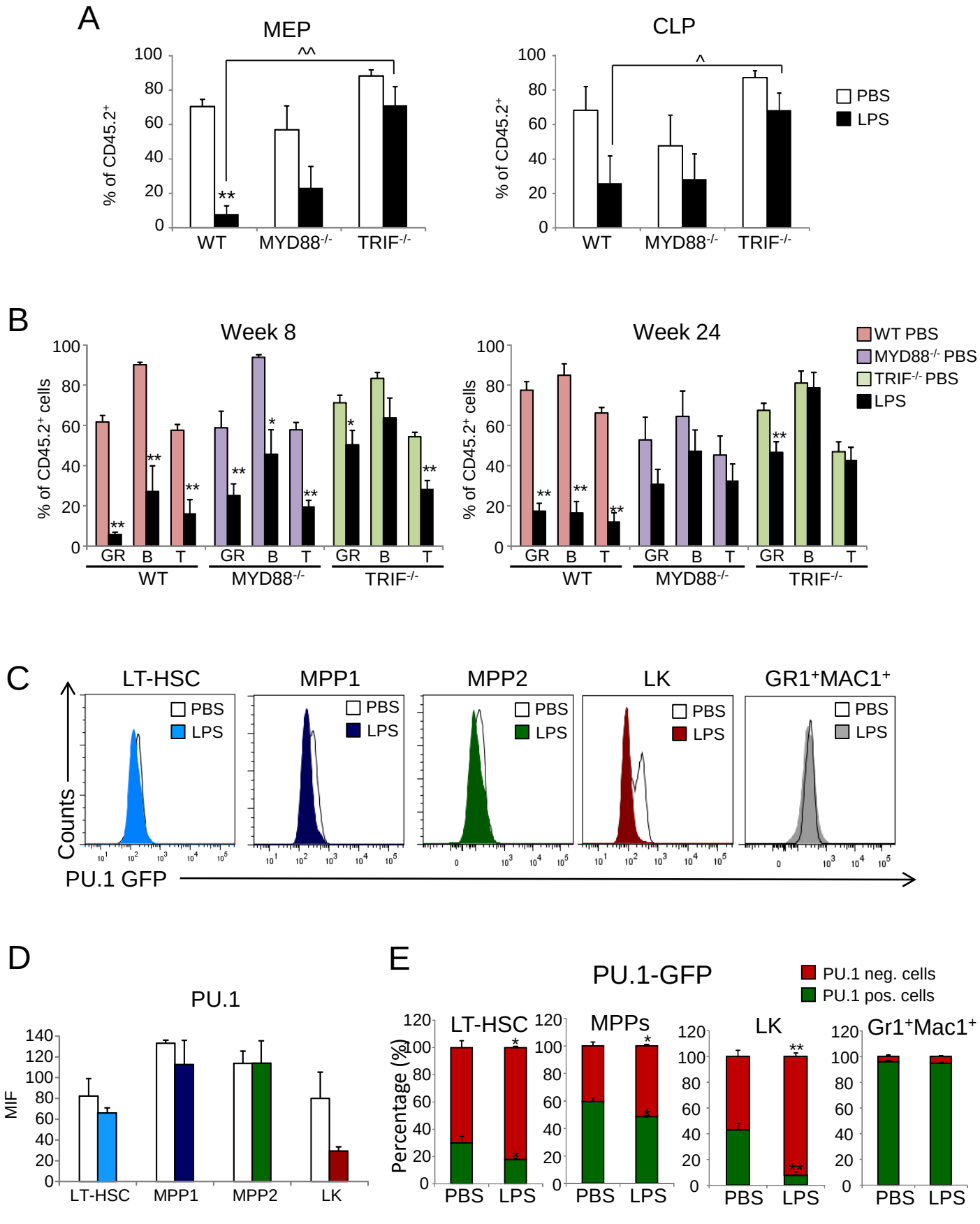
A
MEP
CLP
% of CD45.2+
PBS
LPS
WT
MYD88-/-
TRIF-/-
B
Week 8
Week 24
% of CD45.2+ cells
WT PBS
MYD88-/- PBS
TRIF-/- PBS
LPS
GR
B
T
C
LT-HSC
MPP1
MPP2
LK
GR1+MAC1+
Counts
PU.1 GFP
D
PU.1
MIF
E
PU.1-GFP
PU.1 neg. cells
PU.1 pos. cells
Percentage (%)